International Journal of Earth Sciences

Late Triassic acidic volcanic clasts in different Neotethyan sedimentary mélanges: paleogeographic and geodynamic implication

--Manuscript Draft--

Manuscript Number:	IJES-D-17-00492R3
Full Title:	Late Triassic acidic volcanic clasts in different Neotethyan sedimentary mélanges: paleogeographic and geodynamic implication
Article Type:	Original Paper
Keywords:	Neotethys Ocean; Late Triassic rifting; rift-related magmatism; U-Pb ages; geodynamic model
Corresponding Author:	Szilvia Kövér, Ph.D Magyar Tudomanyos Akademia HUNGARY
Corresponding Author Secondary Information:	
Corresponding Author's Institution:	Magyar Tudomanyos Akademia
Corresponding Author's Secondary Institution:	
First Author:	Szilvia Kövér, Ph.D
First Author Secondary Information:	
Order of Authors:	Szilvia Kövér, Ph.D
	László Fodor
	Zoltán Kovács
	Urs Klötzli
	János Haas
	Norbert Zajzon
	Csaba Szabó
Order of Authors Secondary Information:	
Funding Information:	Országos Tudományos Kutatási Alapprogramok (113013) — Dr László Fodor
	CEEPUS (CIII-RO-0038-12-1617-M-100514) — dr. Szilvia Kövér
Abstract:	U/Pb zircon dating and trace element geochemical analysis were performed on rhyolite clasts of different Middle Jurassic sedimentary mélanges from the Western Carpathian and Dinaric orogen. These igneous clast-bearing sedimentary successions were deposited on the westernmost passive margin of the Neotethys Ocean. During the latest Jurassic and Cretaceous, they became parts of different nappe stacks forming now the Inner Western Carpathians and some inselbergs within the Pannonian Basin. The Meliata nappe was stacked on the northern passive margin, while the Telekesoldal and Mónosbél nappes were part of the imbricated western - south-western margin. U/Pb dating of the 100m-sized blocks and redeposited smaller clasts and fine-grained sediments formed two age groups: 222.6±6.7 and 209.0±9 Ma. Trace element geochemistry suggested within plate continental volcanism as magma source. However, the measured ages are definitely younger than the classic, rift-related Anisian - Ladinian (238-242 Ma) magmatism, which was widespread along the western and south-western margin of the Neotethys Ocean (e.g. Dolomites, different Dinaridic units). On the other hand, similar, Late Triassic ages are reported from tuff intercalations from the Outer Dinarides and Western Carpathians, along with even more sparse effusive rocks of the Slovenian Trough. Trace element (incl. rare earth

	element) analysis showed positive correlation between the mélange clasts and the in situ Late Triassic rhyolites of the Slovenian Trough. This newly established link between the mélange nappes in NE Hungary and the in situ Late Triassic rhyolites in the Slovenian Trough make a good opportunity to reconsider both Middle Jurassic paleogeography, and later tectonic deformations, which led to the separation of the source area and the redeposited clasts.

We have removed all remaining highlited texts, comments and responses. The text is clean.

Late Triassic acidic volcanic clasts in different Neotethyan sedimentary mélanges: paleogeographic and geodynamic implications

Szilvia Kövér[1], László Fodor[1,2], Zoltán Kovács[1,3], Urs Klötzli[4], János Haas[1], Norbert Zajzon[5], Csaba Szabó[3]

[1] *MTA-ELTE Geological, Geophysical and Space Science Research, 1/C Pázmány sétány, H-1117,Budapest, Hungary*, koversz@yahoo.com, +36304320023

[2] *MTA-ELTE Volcanology Research Group*

[3] *Lithosphere Fluid Research Lab at Eötvös University, Budapest, Hungary*

[4] *Department of Lithospheric Research, University Vienna, Vienna, Austria*

[5] *Institute of Mineralogy and Geology, University of Miskolc, Hungary*

Abstract

U/Pb zircon dating and trace element geochemical analysis were performed on rhyolite clasts of different Middle Jurassic sedimentary mélanges from the Western Carpathian and Dinaric orogen. These igneous clast-bearing sedimentary successions were deposited on the westernmost passive margin of the Neotethys Ocean. During the latest Jurassic and Cretaceous, they became parts of different nappe stacks forming now the Inner Western Carpathians and some inselbergs within the Pannonian Basin. The Meliata nappe was stacked on the northern passive margin, while the Telekesoldal and Mónosbél nappes were part of the imbricated western – south-western margin. U/Pb dating of the 100m-sized blocks and redeposited smaller clasts and fine-grained sediments formed two age groups: 222.6±6.7 and 209.0±9 Ma. Trace element geochemistry suggested within plate continental volcanism as magma source. However, the measured ages are definitely younger than the classic, rift-related Anisian – Ladinian (238–242 Ma) magmatism, which was widespread along the western and south-western margin of the Neotethys Ocean (e.g. Dolomites, different Dinaridic units). On the other hand, similar, Late Triassic ages are reported from tuff intercalations from the Outer Dinarides and Western Carpathians, along with even more sparse effusive rocks of the Slovenian Trough. Trace element (incl. rare earth element) analysis showed positive correlation between the mélange clasts and the in situ Late Triassic rhyolites of the Slovenian Trough. This newly established link between the mélange nappes in NE Hungary and the in situ Late Triassic rhyolites in the Slovenian Trough make a good opportunity to reconsider both Middle Jurassic paleogeography, and later tectonic deformations, which led to the separation of the source area and the redeposited clasts.

Keywords

Neotethys Ocean; Late Triassic rifting; rift-related magmatism; U-Pb ages; geodynamic model

Introduction

Clast analysis of a subduction and obduction-related sedimentary complexes provides essential information about the imbricated continental margin and the overriding oceanic crust, both potentially being part of the source area. In active margin setting the great variety of source areas combined with active tectonism, different depositional environments and variable sedimentary processes result in special, 'block-in-matrix' rocks, which are commonly called mélanges (Festa et al 2010a, b and references therein). Both sedimentary and tectonic mélanges were formed in many accretionary orogenic belts during the imbrication of the attenuated continental margin and obduction of the ophiolite nappe.

We examined three sedimentary mélange nappes, which were formed during the Middle Jurassic to Cretaceous closure of the Neotethys Ocean. The onset of ophiolite obduction onto the western – south-western continental margin is relatively well constrained in the Dinarides, Albanides and Hellenides (Dimo-Lahitte et al. 2001). The ophiolite nappes override a tectonic mélange of sheared serpentinite, a sedimentary mélange of Middle to early Late Jurassic in age and the imbricated passive continental margin (e.g. Đerić et al. 2007, 2012; Gawlick et al. 2008, 2017). These relatively well-defined nappes form more or less continuous "belts" from Greece to Bosnia-Hercegovina (Dimitrijević 1982; Schmid et al. 2008).

Tectonised fragments of this nappe system are preserved in NE Hungary, in the Bükk Mts. (Dimitrijević et al. 2003). The basic characteristics of the nappe-pile are rather similar: thin slices of the imbricated passive margin (Bükk nappe system) are overlain by sedimentary mélange nappes (Darnó and Mónosbél nappes). Jurassic gabbro and pillow lavas of the Neotethys Ocean form the uppermost (preserved) nappe slice (Szarvaskő nappe) (Balla et al. 1980; Balla 1983; Csontos 1988, 1999; Haas and Kovács 2001; Kiss et al. 2012; Kovács et al. 2010).

More to the north, the uppermost, thin-skinned nappe system of the Inner Western Carpathians also contains sedimentary mélange nappes, which also derive from a subduction-related basin (trench) of the Neotethys Ocean (Kozur et al. 1996; Kozur and Mock 1997; Mock et al 1998, Kövér et al. 2009a; Aubrecht et al. 2012). Some of these rather small, but important occurrences are also the subject of the recent study. These rocks belong to the Meliata nappe s.s. in Slovakia (Mello et al. 1996) and to the Telekesoldal nappe (TO) in NE Hungary (Grill 1988;

Kövér et al. 2009a, b). The origin and particularly the juxtaposition of the Meliata and TO nappes are subjects to be discussed. It seems to be clear, that they participated together in the mid- to late Cretaceous nappe emplacement of the Western Carpathians, while their original paleogeographic position is still debating.

It is common in all the target sedimentary units that several publications aimed to determine the age of the matrix, and the age, facies and possible source of the different carbonate clasts (Kovács 1988; Mello 1979; Mock et al. 1998; Gawlick and Missoni 2015; Grill 1988; Csontos 1988, 2000; Kövér et al. 2009b). Geochemical characteristics of the basalt and gabbro clasts were also studied (Mock et al. 1998). They were formed in mid-oceanic ridge and back-arc environment, thus they do not carry specific information about the precise location within the strike of the subduction zone.

However, these mélanges contain a large amount of acidic and intermediary volcanic clasts (Csontos 1988; Szakmány et al. 1989), which lack detailed studies in relation to their age, geochemistry or provenance. In the present study, trace element (incl. rare earth element) studies, along with zircon U-Pb dating were performed on rhyolite clasts from three mélange nappes in order to reveal their potential sources.

Geological setting and sample location

The examined volcanic rocks derive from 3 sedimentary mélange nappes which are made up by Middle to Late Jurassic very low to low-grade metasediments. The Meliata and the Telekesoldal nappes belong to the thin-skinned nappe-pile of the Inner Western Carpathians, whereas the Mónosbél nappe is part of the Bükk nappe system (Fig. 1d). The two areas are separated by the Late Oligocene to Miocene Darnó Fault Zone (Zelenka et al. 1983; Fodor et al. 2005), while all structural elements were truncated from their Dinaric continuation by the Late Oligocene–Early Miocene Mid-Hungarian Shear Zone (Fig. 1a) (Csontos and Nagymarosy 1998; Haas et al. 2010b, 2014).

The **Western Carpathians** are the along-strike continuation of the Alpine orogenic system and built up by Apulia-derived far-travelled nappes once belonged to the northern margin of the Meliata oceanic embayment of the Neotethys Ocean (Fig. 1a, 2) (Schmid et al. 2008). The lower part of the nappe-system mainly consists of polymetamorphic crystalline basement rocks with or without preserved Mesozoic cover slices (Fig. 1b). The uppermost part of the nappe-pile consists of several thin-skinned nappe-slices with variable metamorphic overprint (from deep diagenesis to blueschist facies). The sedimentary age of these slices generally ranges from (Carboniferous) Upper Permian to Upper Jurassic. However, the superposition of the different nappes is controversial in the Slovakian and Hungarian literature. Here we will give a short introduction only for the investigated Meliata nappe, and in a later chapter for those nappes, which contain Middle to Upper Triassic igneous rocks.

The **Meliata nappe system** s.l. is made up by the remnants of the oceanic crust and sediments formed in a subduction-related trench of the Triassic–Jurassic Neotethys Ocean (Mock et al. 1998). Based on their metamorphic features, Mello et al (1998) classified the HP/LT blueschist facies part to the Bôrka nappe, whereas the overlying low-grade part to the Meliata nappe s.s. It is to note that in the present contribution we consider Meliata as a low-grade tectono-sedimentary unit, which does not incorporate subduction-related high-pressure metamorphic rocks (e.g. Bôrka unit of Leško and Varga (1980) and Mello et al. 1996, treated also as Meliata in several works, e.g. Faryad 1995). This distinction conforms to more recent structural views (Lexa et al. 2003, Lačný et al. 2016). The Meliata nappe s.s., (in the sense of Mello et al. 1998 and Mock et al. 1998) is considered as a Middle Jurassic tectono-sedimentary mélange accreted to the overlying units during subduction. These units are thin-skinned tectonic slices of low-grade (Turňa/Torna nappe) or non-metamorphosed (Silica) Permian – Jurassic succession. In the investigated Meliata nappe s.s. the most common lithology is dark slate with radiolarite, sandstone and olistostrome intercalations. Based on radiolarians, the age of the radiolarite interbeds is Middle Bathonian to Early Oxfordian (Kozur and Mock 1985; Kozur et al. 1996). The large blocks (olistoliths) are Triassic carbonates, Triassic and Jurassic radiolarites, slightly metamorphosed limestone, siliciclastic rocks, dolomite, radiolarite, rhyolite, basalt, serpentinite. Sample *Mel* derives from a 3 m rhyolite block of the Meliata mélange nappe. It was collected close to Jasov village, where the Meliata nappe is directly overthrust by the uppermost nappe of the nappe pile, the Silica nappe (Fig. 1b). The locality is close to the contact zone.

The structural equivalent of this mélange-like complex is the **Telekesoldal nappe** (TO) in NE Hungary (Csontos 1988; Kövér et al. 2009a). TO nappe also represents a subduction-related complex, composed of black shales, and gravity mass flow deposits: olistostromes and turbiditic sandstones. (Grill 1988; Kovács 1988; Kövér et al. 2009a, b; Deák-Kövér 2012).

The age, the sedimentological features and the predominance of the Middle to Upper Triassic basin facies carbonate clasts within the olistostrome are similar to those of the Meliata nappe. However, there are differences in the composition and particularly in the proportion of the olistostrome components. In the TO metamorphosed limestone clasts are absent, serpentinite clasts are missing and among the volcanic components rhyolite is predominant, while basalt is very rare. The size of the studied rhyolite clasts varies between tens of metres down to crystal fragments. The large, almost 100 m in size rhyolite bodies were considered as subvolcanic intrusions with thermal contact towards the host slate (Máthé and Szakmány 1990). Based on the supposed Jurassic age and basic geochemical data, the rhyolite was interpreted as part of a subduction-related volcanic arc. However, metamorphic petrological studies discarded a thermal contact between rhyolite and host rock, thus its intrusive character became questionable (Kövér et al. 2009a).

Within the TO nappe, samples derive from the following localities and positions. To-1 derives from a 1 m rhyolite olistolith block, which is surrounded by fine-grained, shaley matrix. This type locality of the mélange crops out along the road between Szalonna and Perkupa villages (Figure 1c). The largest known rhyolite body was penetrated by borehole Szalonna Sza-10. We investigated samples from 2 different depth intervals: 124 m (To-2, To-4) and ~55 m (To-3). Another 100 m scale rhyolite body is situated 3.5 km to SW, at the Hunter's house. Sample To-5 was collected from this outcrop.

The other investigated Jurassic metasedimentary complex is part of the Bükk nappe-system (Balla 1983, Csontos 1999). The **Mónosbél nappe** is composed of of Bajocian – Bathonian deep marine siliciclastics, carbonates and siliceous sediments with intercalations of olistostrome beds transported into the basin via gravity mass movements. Along with fragments of acidic and intermediary magmatites, phyllites, siltstones, sandstones, pelagic limestones, radiolarites, and lithoclasts of redeposited oolitic–bioclastic limestones are common in the olistostrome bodies (Csontos 1988, 2000; Pelikán et al. 2005; Haas et al. 2006, 2013). There are detailed studies about the carbonate components, while the knowledge on the volcanic clasts is limited (Haas et al 2013). Sample BüMel derives from a 10 cm large rhyolite olistolith of the Mónosbél mélange, Odvasbükk locality, Bükk Mts (Fig. 1d, 2).

Methods

Radiometric age determinations were carried out on zircon grain separates from different sized rhyolite pebbles and blocks of the TO and Mónosbél mélange nappes. Grain separation and morphological investigations were carried out at the Department of the Mineralogy and Petrology, University of Miskolc (Majoros 2008). Back-scattered electron (BSE) and cathodoluminescence (CL) imaging was performed at the Geological Survey of Austria (Geologische Bundesanstalt) with a Tescan Vega 2 instrument (10 kV acceleration voltage, 0.5 nA beam current, 17 mm working distance).

The LA-ICP-MS analytical work was performed at the Department of Lithospheric Research, University of Vienna in collaboration with the Department of Analytical Chemistry, BOKU. Analytical procedures were identical to the methodology outlined in Klötzli et al. 2009. Zircon 206Pb/238U and 207Pb/206Pb ratios and ages were determined using a 193nm Ar-F excimer laser (NewWave UP193) coupled to a multi-collector ICP-MS (Nu Instruments Plasma). Ablation using He as carrier gas was raster- and spot-wise according to the CL zonation pattern of the zircons. Line widths for rastering were 20-25µm with a rastering speed of 5 µm/sec. Energy densities were 5 – 8 J/cm2 with a repetition rate of 10 Hz. The He carrier gas was mixed with the Ar carrier gas flow prior to the ICP plasma torch. Ablation duration was 60 to 120 sec with a 30 sec gas and Hg blank measurement preceding ablation. Ablation count rates were corrected accordingly offline. Remaining counts on mass 204 were interpreted as representing 204Pb. Static mass spectrometer analysis was as follows: 238U was measured in a Faraday detector, 207Pb, 206Pb, 204 (Pb+Hg), and 202Hg in ion counter detectors, respectively. An integration time of 1 sec was used for all measurements. The ion counter – Faraday and inter-ion counter gain factors were determined before the analytical session using reference zircon Plesovice (Slama et al. 2008). Sensitivity for 206Pb on reference zircon Plesovice was c. 30’000 cps/ppm Pb. For 238U the corresponding value was c. 35'000 cps/ppm U. Mass and elemental bias and mass spectrometer drift of both U/Pb and Pb/Pb ratios, respectively, were corrected applying the "intercept method" of (Sylvester and Ghaderi 1997). The calculated 206Pb/238U and 207Pb/206Pb intercept values, respectively, were corrected for mass discrimination from analyses of reference zircon 91500 measured during the analytical session using a standard bracketing method (Klötzli et al. 2009). The correction utilizes regression of standard measurements by a quadratic function. A common Pb correction was applied to the final data using the apparent 207Pb/206Pb age and the Stacey and Kramers Pb evolution model (Stacey and Kramers 1975). The lower intercept ages are calculated using a forced regeression calculation through 207Pb/206Pb = 0.8± 0.5 (common Pb). Final age calculations were performed with Isoplot© 3.0 (Ludwig 2003). All errors reported for LA data are at the 2-sigma level. Reference zircon Plesovice (Slama et al. 2008) was used as secondary standard in order to test the overall reproducibility of the analytical method. 22 measurements made during the analytical sessions result in a concordia age of 338.1 ± 2.9 Ma. This is within error identical to the accepted reference 206Pb/238U date of 337.13±0.37 Ma (Slama et al. 2008).

We investigated the geochemistry of the studied clasts, and also of the potential in situ magmatic rocks. Trace element content of six samples were analysed at ALS Global Roșia Montană, where 31 elements (Ba, Ce, Cr, Cs, Dy, Er, Eu, Ga, Gd, Hf, Ho, La, Lu, Nb, Nd, Pr, Rb, Sm, Sn, Sr, Ta, Tb, Th, Tl, U, V, W, Y, Yb, Zr) were measured by ICP-MS following acid dissolution after lithium-metaborate fusion. 6 samples were analysed by ACME Lab Ltd. Vancouver by LA- ICP-MS. The target elements were Ba, Ce, Cr, Cs, Dy, Er, Eu, Ga, Gd, Hf, Ho, La, Lu, Nb, Nd, Pr, Rb, Sm, Sn, Sr, Ta, Tb, Th, Tl, Tm, U, V, W, Y, Yb, Zr. 3 samples were analysed by ALS Global

Loughrea by ICP-AES for major elements and ICP-MS for trace elements (Ba, Ce, Cr, Cs, Dy, Er, Eu, Ga, Gd, Hf, Ho, La, Lu, Nb, Nd, Pr, Rb, Sm, Sn, Sr, Ta, Tb, Th, Tm, U, V, W, Y, Yb, Zr).

Results

Radiometric age of the rhyolite clasts and bodies of the Jurassic mélange nappes

Forty-one U-Pb isotope analyses were performed on core and mantle of 31 prismatic zircon crystals. Measured and corrected isotopic ratios are summarized on Table 1.

To-1(1) rhyolite block from the TO mélange (Perkupa-Szalonna road cut key-section)

Within this sample, two age groups can be distinguished. 226.6 ±6.2 Ma old group was measured on the core of an elongated prismatic grain (1-b-a) and two zoned rims (Fig. 3). In case of the 1-c-3 crystal, the 2 billion aged core partly resorbed during a later event, then it was overgrown by this younger zoned rim. There is no sign of dissolution or change in crystallographic orientation between the core and rim of the other grain (1-e-6). The youngest, 206.8 ± 4.9 Ma age was detected on crystals 1-b-1 and 1-a-4. In the latter case there is no age difference within the core and rim of the grain in spite of the visible solution surface separating the two parts (Fig. 3).

To-1(2) and To-1(3) 'matrix' layer of the TO mélange (Perkupa-Szalonna roadcut key-section)

Based on thin section studies the volcanic material was interpreted as redeposited debris (Kövér et al. 2009b) in contrast with the previous interpretations describing these layers as coeval Jurassic tuff horizons (Grill 1988). 222.1±7.9 Ma age was calculated from measurements carried out on the core of two CL-dark crystals (2-a-1 B spot, 3-c-8), on one zoned core (3-c-10) and on two highly zoned overgrowths of the equally oriented cores (2-a-4, 2-a-8) (Fig. 4).

To-2(8) and To-3(7) rhyolite blocks within the TO mélange (core Szalonna Sza-10 ~55m (8) and 124m (7))

Both (7) and (8) samples are from vitroporphyric rhyolite bodies, which were penetrated continuously for tens of meters by borehole Sza-10. 211.6±15 Ma age was calculated from measurements carried out on the cores of three CL-dark crystals (8-c-6, 7-a-5, 8-d-6), on one zoned core (8-a-4) and on two highly zoned overgrowths of the equally oriented cores (7-b-6, 7-d-4) (Fig. 5)

To-5(4) rhyolite body within the TO mélange, at Hunter's house locality

Measurements on 6 crystals with different morphological (elongated or tabular) and CL character yielded ages within the 219.3 ± 6.2 Ma range (Fig. 6). In case of grain 4-b-2 there was no detectable difference in isotopic composition between the CL dark core and the CL light rim in spite of a well-visible solution event between the growths of the two chemically different parts.

BüMel(11), rhyolite block from the Mónosbél nappe (Bükk Mts., Odvasbükk locality)

U-Pb zircon dating of the rhyolite clast deriving from the Mónosbél nappe (Bükk Mts.) resulted in 208.6 ± 10 Ma. Measurements were carried out on the cores of two CL-dark crystals (11-b-5, 11-c-5), on two CL-light cores (11-b-3,11-e-2) and on five highly zoned overgrowths of the equally oriented cores (11-a-4, 11-a-6, 11-d-9, 11-e-5, 11-e-7) (Fig. 7).

The results of the U/Pb age determinations can be summarized as follows. The measurements were carried out on 33 zircon crystals of 7 sample groups. As a result, we have new radiometric age data from different type of the rhyolite occurrences. Such types are fine-grained beds between the olistostrome layers, cm–dm-sized clasts of the olistostrome, and even larger decametric big bodies of disputed position/origin. The results are culminating around two age groups: ~223±7 Ma (late Carnian to Norian) and ~209±9 Ma (Norian to Rhaetian). Both of them indicate volcanic activities in the Late Triassic.

Geochemistry of the rhyolite mélange clasts

Representative chemical compositions of the samples are presented in Table 2 and 3. CaO, Na_2O content and the loss of ignition (LOI) values were very high, while SiO_2 and Al_2O_3 were low in case of the two pebble-size sample (To-1 and BüMel), thus they may not reflect original chemical composition of the magmatic clasts. However, the LOI was not higher than 5% in case of 5 samples. TAS diagram of these ones is indicating rhyolitic composition (Fig. 8).

The majority of the rhyolite clasts (To1-To5) show uniform REE-patterns with a slight enrichment of LREE (Light Rare Earth Element) over HREE (Heavy Rare Earth Element) (LaN/LuN=2.24-4.36) with a pronounced negative Eu-anomaly (2*EuN/(SmN+GdN)=0.17-0.26) (Fig. 9). Two clasts (BüMel and Mel) has higher abundance of LREEs and similar abundance of HREEs compared to the other clasts (LaN/LuN=6.27 and 7.69, respectively), therefore a bit higher Eu-anomaly as well (2*EuN/(SmN+GdN)=0.5 and 0.3, respectively) (Fig. 9a).

N-MORB normalized multi-element diagram show a continuous decrease in abundance from the incompatible trace elements to the more compatible ones (e.g. Th has 100-fold enrichment, while HREEs are showing N-MORB values or maximum 2-fold enrichment). Negative anomalies are observed in case of Nb, Eu, Sr and Ti (Fig. 10a, b).

Discussion

Age of the mélange-related rhyolites and their interpretation

In the Rudabánya Hills, TO nappe, the calculated magmatic ages of the rhyolite bodies significantly differ from the previously suggested Late Jurassic age of Szakmány et al. (1989) while support the olistolith interpretation (Kövér et al. 2009a, b). Thus, the Late Triassic volcanic clasts are olistoliths (large clasts) – independently of their size – within the Middle Jurassic slate matrix.

The main problem of the measured clast ages (~223±7 Ma and ~209±9 Ma) is the age itself. They are considerably younger than the typical 238-242 Ma Middle Triassic Neotethyan rift-related magmatic ages (Fig. 11), which are reported from those structural units, which formed the south-western and western passive margin of the Neotethys Ocean (Mundil et al. 1996, Pálfy et al. 2003, Wotzlaw et al. 2018). On the other hand, there are sporadic radiometric and stratigraphic data referring to less wide-spread magmatic events during the Late Triassic (for details, see next chapters). Effusive rocks with Late Triassic radiometric or stratigraphic age are present in the Dolomites and Slovenian Trough – Julian Alps, tuff horizons were described from the Outer Dinarides (Pamić and Lovrić 1980; Pleničar et al. 2009; Neubauer et al. 2014), while zircon grains in tuffitic redeposited layers were reported from the Western Carpathians (Kohút et al. 2017). These occurrences support a Late Triassic magmatic event at the western termination of the Neothetys embayment. The main centre for this volcanism should have been located at the western termination or along the south-western margin of the ocean, while the northern, Western Carpathian margin received only very fine grained tuff supply. On the other hand, lava rocks and dykes are present in the Southern Alps and Dinarides, deriving from the south-western margin (Fig. 2).

Possible sources of the redeposited volcanic clasts of the Telekesoldal and Mónosbél sedimentary mélange nappes

On the basis of the newly obtained ages, we supposed that the source of the investigated clasts was a Late Triassic volcanic field. To establish a genetic link between the clasts and possible sources, we briefly introduce the in-situ Late Triassic effusive rocks and tuffs, and compare to our samples.

Central Western Carpathians

Only siliciclastic sediments with syn-depositional magmatic source indicate volcanic activity in the Late Triassic succession of any Western Carpathian nappes (Kovács et al. 2011; Kohút et al. 2017). The Upper Triassic, siliciclastic Lunz Formation yielded detrital zircons with 221.2 ±1.6 Ma age (Kohút et al. 2017). These detrital ages were interpreted as the maximum age of sedimentation, thus the source of these zircon grains was a co-existing volcanic activity. The age interval is overlapping the older age group of our dated olistoliths (Fig. 11). However, these zircon grains were redeposited as single grains, and may derive from distantly located volcanic edifices thus the Lunz Formation itself cannot be the direct source of the mélange clasts.

Southern Alps, Dinarides, Slovenian Trough

The Dolomites of the Southern Alps along with the Dinarides are the classical localities of the Middle Triassic syn-rift volcanic activity. During the latest Anisian to early Ladinian rifting of the Neotethys Ocean tilted blocks were developed with carbonate platforms and narrow intraplatform basins. Volcanoclastic intercalations (‘Pietra Verde’) predominantly occur in the deeper water Buchenstein Fm. These volcanoclastics are products of an explosive, acidic volcanism. Their wide spatial distribution suggests that a number of volcanic centres existed throughout the western termination of the Neotethys Ocean (Castellarin et al. 1998). The age of the main magmatic phase was between 238-242 Ma (Mundil et al. 1996, Wotzlaw et al. 2018), thus definitely older than the investigated rhyolite clasts (Fig. 11). However, there are sporadic indications of a younger magmatic episode. Németh and Budai (2009) and Budai et al. (2004) reported breccia pipes cross-cutting the Ladinian platform carbonate (Schlern Dolomite). K/Ar age (204±7.8 Ma) of the diatreme is much younger than the classic syn-rift magmatic event (Budai et al. 2004). These indices may hint that magmatism could continue, at least locally, into the Late Triassic. However, the lithology (breccia pipes in the Dolomites vs. rhyolite lava rocks within the clasts) does not allow direct source – clast link between this occurrence and the investigated mélange clasts.

“Tuffaceous breccia” and sandstone are also described from the Carnian siliciclastic intercalations from the Outer Dinarides (Slivnica) (Pleničar et al. 2009). The tuff is promising, however, effusive rock is needed for a direct comparison.

Explosive magmatic activity post-dating the main Middle Triassic magmatic event is also present in some regions of the Outer Dinarides (Northern Croatia) (Pamić and Lovrić 1980). Carnian and Norian ages of the effusive rocks are supported by stratigraphy and Rb/Sr data (223±7 Ma). New findings of Neubauer et al. (2014) from the Julian

Alps and the Slovenian Trough strengthen magmatic activity during the Carnian – Norian (223.7±1.5 Ma, 233.7±1.5 Ma). The younger ages are in positive correlation with the age of the mélange clasts, thus we continued with geochemical analysis.

Geochemical data of in situ Late Triassic rhyolites

While both the rhyolitic lithology and the age data allowed possible match with the mélange clasts, we took three samples of two localities for comparative geochemical study. Sample SLO-1 was collected from the Lajše locality, which was dated as 223.7±1.5 Ma by Neubauer et al. (2014). It is a greenish-grey rhyolite with plagioclase phenocrysts. Sample SLO-2 is a rhyolite tuff, which intercalates with Late Triassic marl and clastics (Grad et al. 1974).

Representative chemical composition of the three samples is shown in Table 2 and 3. The rhyolites: SLO1 and SLO2 (Fig. 8) have very high (74 and 81 wt. %) SiO_2-, and exceptionally low $MgO+Fe_2O_3$ content (3.2 and 2.1 wt. %, respectively). LOI values were low (1-3.5 wt. %).

The Slovenian samples have REE- and multielement patterns similar to the rhyolite clasts of the mélange (Fig. 9a, 10a, b), showing LREE enrichment over HREE (La_N/Lu_N=8.85 and 9.53), Eu-anomaly ($2*Eu_N/(Sm_N+Gd_N)$=0.31 and 0.32, respectively), and a continuous decrease from incompatible to compatible trace elements normalized to N-MORB (Fig. 10a,b.). Negative Nb, Sr, Eu and Ti-anomalies are also present.

All these geochemical data strengthen the similarity between the in situ rhyolite and rhyolite tuff and the dated clasts from the mélange units. The similar age (Fig. 11) and trace element geochemistry raise the Late Triassic rhyolites of the Slovenian Trough to a potential source area for the mélange clasts.

Tectonic framework of the Late Triassic rhyolite volcanism on the basis of trace element geochemistry

Geodynamic evaluation of the rhyolite samples is investigated based on the system of Furnes & Dilek (2017). Patterns of REE and immobile trace elements (Th, Nb, La, Ce, Sr, Nd, Zr, Sm, Eu, Gd, Ti, Dy, Y, Yb, Lu) are considered along with La_N/Lu_N-ratios in the determination of the paleogeotectonic setting. Inclining REE-patterns (with or without Eu-anomaly) occur in every type of igneous suite, as it is a general feature of the more fractionated (intermediate to acidic) magmas (Fig. 9a). In contrast, immobile trace element patterns are more characteristic, negative Nb, Sr, Eu and Ti-anomalies are characteristic for igneous suites of Rift/Continental Margin- (R/CM) and Plume/MOR (P/M) type (Fig. 10a). Negative Sr- and Eu-anomalies might be interpreted as a signature of early fractionation during magma evolution, where plagioclase locks away Sr and Eu form the melt. Relative Sr-enrichment of BüMel and To1 samples may be related to weathering processes, where carbonates collect Sr from fluids interacting with the exposed rocks. This is strengthened by high LOI values (8.71 and 10.7, respectively). Partition coefficient of Nb and Ti is sensitive to the H_2O-content of the melt, as they are more compatible in H_2O -rich magmatic systems. Therefore, they tend to segregate in the early fractionates, or even remain in the solid component during the melting of the mantle material, if H_2O is present during melting. Zr has slightly lower concentration compared to the average R/CM and P/M magmas (1-3,5-fold enrichment instead of 3-10-fold enrichment compared to N-MORB), but this may be related to local characteristics of the original mantle material. Further discrimination would be possible based on the distribution of La_N/Lu_N ratios (Fig. 9b) . However, the small amount of data does not show a characteristic distribution, as all of the points are between 2 and 10, as in the case of both R/CM and P/M magma types.

The Th/Yb-Ta/Yb diagram of Gorton and Schandal (2000) was also made to discriminate between acidic rocks of different tectonic origin. Elevation of Th/Yb-ratio implies addition of crustal material via subduction, while the Ta/Yb ratio is depending on the degree of partial melting of the mantle (higher values indicate lower ratio of partial melting). The clasts from the different mélange nappes are characterized as within plate volcanic rocks, while the Late Triassic Slovenian samples are plotted in the boundary between the within plate and the adjacent active continental margin area (Fig. 10c.).

The combined occurrence of the negative anomalies of Nb, Sr, Eu and Ti and the relatively low La_N/Lu_N-ratios suspect a subduction-unrelated, yet H2O-rich magma of within plate origin. Rift/Continental Margin-type volcanism as a source of the rhyolite clasts of the mélange and also for the in situ Slovenian volcanites is suggested. It needs further analysis to find out the plate tectonic background of this rifting. As preliminary models, two potential events can be suggested; (1) continuation/renewal of the Middle Triassic Neotethyan rifting and continental rift-related magmatism (2) far-field echo of the earliest continental phase of the Alpine Tethys (Penninic) rifting. In case of (1), the large time lag with respect to break-up represents a problem, while in solution (2) the large distance from known rift axis (oceanic spreading centre) needs explanation. The Atlantic-related break-up of the Piemont – Ligurian branch of the Penninic Ocean was preceded by a long continental rifting phase, which affected the whole Adriatic crust. Radiometric ages from the main shear zones of the Ivrea-Verbano zone (representing the exhumed and thinned Adriatic crust) indicates high temperature deformation and thinning of the lower and middle crust from 210 Ma (latest Triassic) (Wolff et al. 2012, Langona et al. 2018), while extensional sedimentary basins in the Southern Alps (Lombardian Basin, Belluno Basin, Slovenian Trough), Northern Calcareous Alps (Bajuvaric nappes,) and Transdanubian Range (Zala Basin) documents the upper crustal extension from early Norian (228 Ma) (Bertotti et al. 1993, Behrmann and Tanner 2006, Goričan 2012, Héja et al. 2018). Later on, during the Early and Middle Jurassic the depocentre of extensional deformation was migrated westward, towards the future Alpine Tethys.

Plate tectonic consequences

Middle Jurassic: Potential source areas and paleogeography

While potential source areas of rhyolite clasts can be suggested (Slovenian Trough) and others can be excluded (northern margin of Neotethys), it gives a possibility to suggest modifications (refinements) for existing Mesozoic paleogeographic and plate tectonic models. During the Triassic – Late Jurassic interval, the Transdanubian Range, the future Austroalpine nappes, the Dolomites and the Slovenian Trough were located at the terminating western embayment of the ocean, while the sub-ophiolitic units of the Dinarides (together with the future Bükk and Mónosbél nappes) formed the south-western passive margin (Fig. 2, Fig12) (Dercourt et al. 1990; Kozur 1991; Haas et al. 1995; Stampfli and Borel 2002; Csontos and Vörös 2004; Velledits 2006; Schmid et al. 2008; Handy et al. 2010). In contrast, those structural units, which build up the present day Western Carpathians are generally placed north or northeast from the TR, thus onto the northern margin of the Neotethys (Haas et al. 1995; Plašienka 1998).

Units from the south-western (Adriatic-Dinaric) margin: Mónosbél mélange nappe, TO nappe

The footwall of the **Mónosbél nappe**, the Bükk nappe (Fig. 1d) was always considered as deposited on the SW Dinaridic margin (Kovács et al. 2011; Csontos 2000; Haas et al. 2011a), although the exact position of the Bükk is still not fully constrained; it varies from near-reef-slope Zlambach facies zone of Gawlick et al. (2012), to more ocean-ward proximal zones (Schmid et al. 2008). The overlying Mónosbél unit is generally considered as a nappe (Csontos 1999), although a continuous succession from the Bükk nappe cannot be completely ruled out (Pelikán et al. 2005). Recent sedimentological studies clearly indicate that this area received considerable amount of clasts from the Adriatic Dinaric Carbonate Platform (ADCP) during the Middle Jurassic (e.g. Mid-Jurassic ooidal limestone and skeletal fragments) (Haas et al. 2006, 2011b). Thus the presumed paleogeographic position (Fig. 12) must be relatively close to the ADCP, but the exact along-strike position cannot be defined more precisely (on the basis of Jurassic clast-source connection). On the other hand, the now-described Triassic volcanic fragments can be reconciled with a potential source from the Slovenian Trough, or from the eastern part of the Julian Alps;

this northerly position, at the eastern continuation of the Slovenian Trough would permit a much shorter transport route for rhyolite clasts., This paleoposition would also permit an easier juxtaposition of the Bükk nappe pile and TR units, and their amalgamation into a common Cenozoic tectonic unit (ALCAPA on Figure 1).

In the Rudabánya Hills (Fig. 1c), clast composition of the **TO sedimentary mélange nappe** is dominated by pelagic limestones and marlstone derived from the thinned margin; basalts are rare. The investigated large rhyolite clasts connect this sedimentary mélange-like unit to the SW margin, more precisely, to the vicinity of the Slovenian Trough (Fig. 12). Other elements in the Rudabánya nappe pile also support this paleogeographic location. The TO nappe is thrust over the Bódva unit, which contains a relatively deep water (outer shelf) Triassic succession, which is more similar to Dinaridic units than to some potential Eastern Alpine or Western Carpathian facies (Kovács et al. 1989, 2011; Gawlick et al. 2012). The rare Ammonite fauna also correlate the Bódva unit more with the south-western, than the northern attenuated margin (Vörös 2010). Finally, its Middle Jurassic formations contain coeval platform-derived fossils and clasts (Kövér et al. 2009b), which anchors the position of Bódva close to the Adriatic Dinaric Carbonate Platform (ADCP on Fig. 12).

Units from the north-eastern (Western Carpathian) margin? Meliata mélange nappe

In the present day Inner Western Carpathians, the most characteristic nappe is the subduction related high-pressure Bôrka unit (Faryad 1997, Faryad et al. 2005). The associated metamorphism is well constrained between 160–150Ma (Maluski et al. 1993; Dallmeyer et al. 1996, 2008; Faryad and Henjes-Kunst 1997). The blueschist-facies metamorphism is roughly coeval with the age of sedimentation in the sedimentary mélanges. From kinematic indicators, the direction of subduction was towards the south, thus once it represented the north-eastern passive margin of the Neotethys Ocean. The Meliata mélange was deposited in a trench between the southward subducting Inner Western Carpathian thinned margin and the overriding ophiolite unit and its frontal imbricates (Plašienka 1997, 1998; Plašienka et al. 1997; Less 2000; Ivan 2002; Lexa et al. 2003; Dallmeyer et al. 2008). These models agree that tectonic burial, metamorphism and exhumation of the trench-derived Meliata nappes were also related to this southward subduction but occurred later, possibly in the earliest Cretaceous (Árkai et al. 2003).

The origin of most carbonatic and basic-ultrabasic magmatic clasts of the Meliata mélange can fit to this model, while they could derive from the overriding ophiolite, or scrapped off from the down-going Triassic oceanic slab. The great variety of shallow to deep-water Triassic carbonate clasts could be available on the underthrusting (northern) passive margin or from slivers attached to the overriding ophiolitic units.

Late Jurassic to Early Cretaceous strike-slip faulting

The present-day close disposition of the Meliata and TO units either require (1) original close paleogeographical position, only slightly modified by nappe stacking, or (2) important displacement during or after nappe stacking of the two mélange units. The rhyolite clasts present in both units permit but not unequivocally confirm the first solution. (2): large-scale displacement of a formerly SW margin-related units (TO, Bódva) could be possible via strike-slip faults.

Such sinistral major fault or fault zone was postulated in the Eastern Alps. First, we briefly discuss these ideas then explain how it helps solving some problems of the Inner Western Carpathians.

Present-day arrangement of characteristic Late Triassic facies-belts in the Eastern and Southern Alps is not in agreement with a linear or convexly curved passive margin of the Neotethys Ocean. The present-day general trend in the NCA is that in a N-S section the northern (deeper) nappe-slices represents more proximal, while the southern nappe-slices more distal segments of the Triassic passive margin. This geometry is partly due to the E-W strike of the nappes. However, the Dachstein facies zone terminates towards the W in the western part of the NCA. In contradiction, the same lagoon - platform facies boundary (Dachstein Limestone – Hauptdolomite) is located much more to the east in the Transdanubian Range. This led Kázmér and Kovács (1985) to suggest sinistral slip along the north-western and northern boundary of the TR (although they erroneously considered this movement as Cenozoic). The same kinematics was suggested by Schmidt et al. (1991), shifting the westernmost, marginal part of the Neotethyan embayment (including TR) towards the east. They suggested Middle Jurassic – Early Cretaceous timespan for the movement, and a kinematic link towards the opening Ligurian-Piemont Ocean.

This postulated sinistral fault is also shown in paleotectonic reconstruction of Schmid et al. (2008), Handy et al. (2010) where this fault was named as the proto-Periadriatic Transform line. Moreover, the initiation of the intra-continental subduction within the Austroalpine nappe-system was suggested to be the result of this same sinistral transfer fault, juxtaposing continental blocks with different crustal thicknesses (Stüwe and Schuster 2010).

Following these data, concepts and interpretations, we also suggest, that the western embayment of the Neotethys could be dissected by several sinistral transfer faults (Fig. 12). The northern fault could have controlled the E-W striking intra-continental subduction in the East-Alpine domain, and may have played a role in the subsequent mid—Cretaceous contraction (Stüwe and Schuster 2010; Janák et al. 2001).

The delimited blocks contain the Ötztal-Bundschuh basement, the future Silica nappes, the TR, and involved the future Meliata nappe s.str (Fig. 12). The sinistral slip could be dissipated at the subduction front (e.g. Schmid et al. 2008; Handy et al. 2010), but also could cut off obducted ophiolite blocks. This latter version would trap obducted ophiolite blocks within the subsequently forming Eo-Alpine nappe stack.

One of the useful consequences of sinistral faulting would be the southerly position of Silica nappe with respect to the juxtaposing Meliata-Bôrka assemblage (Fig. 12b). The northern-margin origin of Silica (e.g. Plašienka et al. 1997; Kovács et al. 1989, 2011; Less 2000; Schmid et al. 2008) would imply a lower plate position during the southward WC subduction, however, its non-metamorphic character and uppermost tectonic position would suggest upper plate origin. This contradiction puzzled plate-tectonic reconstructions in the WC for a long time (see Plašienka et al. 1997; Plašienka 1998). The sinistral shift of Silica unit prior to the completion of the Inner Western Carpathian nappe pile would result in an upper plate position with respect to the subduction (Fig. 12). This version already suggested by Deák-Kövér (2012), can be an alternative model to the triangle structure of Schmid et al (2008). Minor sinistral displacement zones within the Silica nappe is supported by local observations and mapping (Ménes Valley, Grill et al. 1984; Less et al. 1988; Less 2000).

Timing

The sinistral faulting has slightly varying time frame in different works. Schmidt et al. (1991) postulated continuous transform movements from Middle Jurassic to Early Cretaceous, while a kinematic link was suggested between the opening of the Piemont – Ligurian ocean and the transfer fault. Stüwe and Schuster (2010) suggested movements postdating the obduction (post 170-160 Ma) and predating the onset of Eoalpine metamorphism (135 Ma). According to the work of Frank and Schlager (2006), this important deformation was coeval with late Middle to early Late Jurassic tectonically controlled sedimentation of the Northern Calcareous Alps (Ortner 2017).

In our model, the main argument for timing is the age of the sedimentary mélanges and the juxtaposition of the Meliata and Bôrka units. Our model would suggest syn- to post- late Middle Jurassic displacement. Meanwhile, the juxtaposition of the Meliata and Bôrka unit could suggest an upper age limit to this deformation. K-Ar ages of Meliata sensu stricto metasediments range from ~145 to 128 Ma (Árkai et al. 2003). K-Ar white-mica ages may indicate the peak metamorphic condition or initial cooling for the low-grade Meliata. Separation of these two events is difficult, while the maximum temperature condition of Meliata metamorphism is close to the closure temperature of the K-Ar system. K-Ar cooling ages of the high-pressure Bôrka unit are in the same age interval on the basis of K-Ar mica dating (Árkai et al. 2003). However, more recent EMPA monazite ages enables narrowing of this range to 145-140 Ma (Méres et al. 2013); meaning juxtaposition of Meliata and Bôrka nappes in this time span.

In conclusion, we prefer a wide time range, from late Middle Jurassic to early Cretaceous (~168 Ma – ~140 Ma), which may be narrowed by further assumptions in future.

Conclusion

A few mm to 100 m sized rhyolite clasts and blocks were investigated from different Middle Jurassic Neotethyan sedimentary mélange nappes. New U-Pb isotopic data from zircon grains proved that the age of rhyolite clasts forms two age groups: 222.6±6.7 and 209.0±9 Ma. These Late Triassic ages are in contradiction with previous interpretations of a Middle Jurassic, subduction-related island arc origin. In contrast, even the largest (ca. 100-150 m) rhyolite bodies are redeposited Late Triassic magmatic rocks within the Middle Jurassic sedimentary matrix.

The calculated age groups (222.6±6.7 and 209.0±9 Ma) do not fit into the general Late Anisian – Ladinian (~242-238 Ma) magmatism, which was a wide-spread magmatic event on the south-western passive margin of the opening Neotethys Ocean. However, both geochemical REE and trace element pattern and U/Pb zircon age show positive correlation between the clasts and in situ Late Triassic rhyolite and rhyolite tuff from the Slovenian Trough. Selected trace element and REE pattern suggest subduction-unrelated, most probably Rift/Continental Margin-type volcanism as plate tectonic setting for the Late Triassic magma. Due to the rather large (~20 Ma) time gap, we prefer connecting this magmatism rather to the early, continental thinning of the Penninic rifting, than to the elongation/renewal of the Neotethyan one.

While the most probable source of the rhyolite clasts, the Slovenian Trough was located on the south-western passive margin of the Neotethys Ocean, depositional area of the TO and Mónosbél mélange nappes should have been close to this area, while long-distance transportation of the large clasts toward the northern margin is less probable option. Thus we suggest the following model: deposition of the TO and Mónosbél Middle Jurassic sedimentary mélanges took place on the south-western passive margin of the Neotethys Ocean. Shortly after the sedimentation, branches of a large-scale, roughly E-W-striking sinistral fault zone made considerable rearrangement of the stacked ophiolite, sub-ophiolitic mélange and imbricated passive margin nappes. As a result, the northern, Western Carpathian margin was juxtaposed directly with some fragments of the imbricated south-western margin, e.g. TO and Mónosbél units. During this process, the Meliata sedimentary mélange and the exhuming high-pressure Bôrka nappe can get in tectonic contact. A southern branch of this post-obductional sinistral shear-zone would shift the Silica area to a southern, opposing position with respect to the Meliata-Bôrka nappe system and the more proximal Western Carpathian margin. Subsequent mid-Cretaceous nappe-stacking could result in out-of-sequence thrusting of the Silica nappe as a higher unit onto the Meliata-Bôrka system and, together, further to the N onto other Western Carpathian units.

Acknowledgement

Sampling, U-Pb and geochemical measurements was supported by the Hungarian National Science Fund (OTKA) grant number K 113013 and Slovenian CEEPUS scholarship of Sz. Kövér. Useful comments and questions of Dušan Plašienka and an anonymous reviewer highly improved the manuscript.

References

Árkai P, Faryad SW, Vidal O, Balogh K (2003) Very low-grade metamorphism of sedimentary rocks of the Meliata unit, Western Carpathians, Slovakia: implications of phyllosilicate characteristics. Int J of Earth Sci 92: 68-85.

Aubrecht R, Gawlick H-J, Missoni S, Plašienka D (2012) Meliata type locality revisited: Evidence for the need of reinvestigation of the Meliata Unit and redefinition of the Meliata Mélange. Mineralia Slovaca, 44 Web ISSN 1338-3523, ISSN 0369-2086

Balla Z. (1983): A szarvaskői szinform rétegsora és tektonikája. Annu. Rep. Eötvös Loránd Geophysical Inst of Hung, 1982, 42–65.

Balla Z, Baksa Cs, Földessy J, Havas L, Szabó I. (1980) The tectonic setting of ophiolites in the Bükk Mountains (North Hungary). Geologicky Zbornik–Geologica Carpathica 31/4: 465–493.

Behrmann JH, Tanner DC (2006) Structural synthesis of the Northern Calcareous Alps, TRANSALP segment. Tectonophysics 414:225–240.

Bertotti G, Picotti V, Bernoulli D, Castellarin A (1993) From rifting to drifting: tectonic evolution of the South-Alpine upper crust from the Triassic to the Early Cretaceous. Sedimentary Geology 86(1–2):53–76. http://doi.org/10.1016/0037-0738(93)90133-P

Budai T, Németh K, Piros O (2004) Middle Triassic platform carbonates and volcanites in the Latemar area (Dolomites, Italy). Annu Rep of the Hung Geol Inst, 2004 175-188. (in Hungarian with English abstract)

Castellarin A, Lucchini F, Rossi PL, Selli L, Simboli G (1988) The middle Triassic magmatic-tectonic arc development in the southern Alps. Tectonophysics, 146: 79-89.

Csontos L (1988) Etude géologique d'une portion des Carpathes Internes, le massif du Bükk (Nord-est de la Hongrie), (stratigraphie, structures, métamorphisme et géodinamique). Ph. D. thesis, University Lille Flandres-Artois, n° 250, pp 327

Csontos L (1999) Structural outline of the Bükk Mts. (N Hungary). Földtani Közlöny 129/4: 611–651 (in Hungarian with English abstract).

Csontos L (2000) Stratigraphic reevaluation of the Bükk Mts (N. Hungary). Földtani Közlöny 130: 95-131 (in Hungarian with English abstract).

Csontos L, Nagymarosy A (1998) The Mid-Hungarian line: a zone of repeated tectonic inversion. Tectonophysics, 297: 51–72.

Csontos L, Vörös A (2004) Mesozoic plate tectonic reconstruction of the Carpathian region. Palaeogeography, Palaeoclimatology, Palaeoecology 210: 1–56.

Dallmeyer RD, Neubauer F, Handler R, Fritz H, Müller W, Pana D, Putiš M (1996) Tectonothermal evolution of the internal Alps and Carpathians: Evidence from 40Ar/39Ar mineral and whole-rock data, Eclogae Geol Helv 89: 203-227.

Dallmeyer RD, Neubauer F, Fritz H (2008) The Meliata suture in the Carpathians: regional significance and implications for the evolution of high-pressure wedges within collisional orogens, in: Siegesmund S., Fügenschuh B., Froitzheim N. (eds.), Tectonic Aspects of the Alpine-Dinaride-Carpathian System, Geol Soc, Sp Publ 298, pp 101-115.

Deák-Kövér Sz (2012) Structure, metamorphism, geochronology and deformation history of Mesozoic formations in the central Rudabánya Hills. PhD dissertation, Eötvös University, Budapest pp 162.

Dercourt J, Ricou LE, Adamia S, Csfiszfir G, Funk H, Lefeld J, Rakfs M, Sandulescu M, Tollmann A, Tchoumachenko. P (1990) Anisian to Oligoccne paleogeography of the European margin of Tethys (Geneva to Baku). Mém Soc Géol France. 154: 159-190.

Dimitrijević M (1982) Dinarides: an outline of the tectonics: Earth Evol. Sci, 1: 4-23.

Dimitrijević MN, Dimitrijević MD, Karamata S, Sudar M, Gerzina N, Kovács S, Dosztály L, Gulácsi Z, Less Gy, Pelikán P (2003) Olistostrome/mélanges — an overview of the problems and preliminary comparison of such formations in Yugoslavia and NE Hungary. Slovak Geol Mag 9/1: 3–21.

Dimo-Lahitte A, Monié P, Vergély P (2001) Metamorphic soles from the Albanian ophiolites: petrology, 40Ar/39Ar geochronology, and geodynamic evolution. Tectonics 20: 78–96.

Đerić N, Gerzina N, Schmid MS (2007) Age of the Jurassic radiolarian chert formation from the Zlatar Mountain (SW Serbia). Ofioliti 32/ 2: 101–108

Đerić N, Schmid SM, Gerzina N (2012) Middle Jurassic radiolarian assemblages from the sedimentary cover of the Adriatic margin (Zlatar Mountain, SW Serbia). Bull Soc Géol France 183/4

Faryad SW (1995) Phase petrology of mafic blueschists of the Meliata Unit (Western Carpathians) – Slovakia. J Metamorph Geol 13:432–448.

Faryad SW (1997) Lithology and metamorphism of the Meliata unit high-pressure rocks. In: Grecula P, Hovorka D, Putis M (eds) Geological evolution of the Western Carpathians. Mineralia Slovaka Corp Geocomplex as Geol Surv Slovak Republic, Bratislava, pp 131–144.

Faryad SW, Henjes-Kunst F (1997) K-Ar and Ar-Ar age constraints of the Meliata blueschist facies rocks, the Western Carpathians (Slovakia). Tectonophysics 280:141–156.

Faryad SW, Spišiak J, Horváth P, Hovorka D, Dianiška I, Józsa S (2005) Petrological and geochemical features of the Meliata mafic rocks from the sutured Triassic oceanic basin, Western Carpathians. Ofioliti 30: 27-35.

Festa A., Pini GA, Dilek Y, Codegone G (2010a). Mélanges and mélange forming processes: historical overview and new concepts. International Geology Review 52, 1040–1105

Festa A, Pini GA, Dilek Y, Codegone G, Vezzani L, Ghisetti F, Lucente CC, Ogata K (2010b) Peri-Adriatic mélanges and their evolution in the Tethyan realm. International Geology Review 52: 369–406

Fodor L., Radócz Gy., Sztanó O., Koroknai B., Csontos L. & Harangi Sz. 2005. Tectonics, sedimentation and magmatism along the Darnó Zone. Post-Conference Excursion Guide for 3rd Meeting of the Central European Tectonic Studies Group, Felsőtárkány, Hungary. Geolines 19: 142–162.

Frank W, Schlager W (2006) Jurassic strike slip versus subduction in the Eastern Alps. Int J Earth Sci 95: 431-450.

Fuchs W (1984) Geotektonische neuorientung in den Ostalpen und Westkarpaten unter Einbeziehung plattentektonischer Gesichtpunkte. Jahrbuch der Geologischesen Bundesanstalt 127/4: 571-632.

Furnes H, Dilek Y (2017) Geochemical characterization and petrogenesis of intermediate to silicic rocks in ophiolites: A global synthesis. Earth-Sci. Rev. 166:1-37.

Furrer H, Schaltegger U, Ovtcharova M, Meister P (2008) U-Pb zircon age of volcaniclastic layers in Middle Triassic platform carbonates of the Austroalpine Silvretta nappe (Switzerland). Swiss J of Geosci, 101/3: 595-603

Gawlick H-J, Missoni S (2015) Middle Triassic radiolarite pebbles in the Middle Jurassic Hallstatt Mélange of the Eastern Alps: implications for Triassic-Jurassic geodynamic and palaeogeo-graphic reconstructions of the western Tethyan realm. Facies 61/ 3: 13.

Gawlick H-J, Frisch W, Hoxha L, Dumitrica P, Krystyn L, Lein R, Missoni S, Schlagintweit F (2008) Mirdita Zone ophiolites and associated sediments in Albania reveal Neotethys Ocean origin. Intern J Earth Sci 9: 865–881

Gawlick H-J, Missoni S, Schlagintweit F, Suzuki H (2012) Jurassic active continental margin deep-water basin and carbonate platform formation in the north-western Tethyan realm (Austria, Germany). J Alp Geol 54: 89-292.

Gawlick H-J, Sudar MN, Missoni S, Suzuki H, Lein R, Jovanovic D (2017) Triassic – Jurassic geodynamic history of the Dinaric Ophiolite Belt (Inner Dinarides, SW Serbia). J Alpine Geol 55: 1-167.

Goričan S (2012) Mesozoic deep-water basins of the eastern Southern Alps (NW Slovenia). IAS Field Trip Guidebook, 101–143.

Gorton MP, ES Schandal (2000) From continents to Island arcs: a geochemical index of tectonic setting for arc-related and within-plate felsic to intermediate volcanic rocks. The Canadian Mineralogist, 38: 1065–1073

Grad K, Ferjančič L, Buser S, Cimerman F, Doset S, Mioč P, Premru U, Vujič D, Žlebnik L, Žnidarčič M (1974) Basic Geological Map of Former Yugoslavia 1:100000, Sheet L 33-65 Kranj, Institute for Geological and Geophysical Research, Belgrade (in Serbian)

Grill J (1988) Jurassic formations of the Rudabánya Mts. Ann Rep Hung Geol Inst, 1986, 69–103 (in Hungarian with English abstract).

Grill J, Kovács S, Less Gy, Réti Zs, Róth L, Szentpétery I (1984) Geology and evolutionary history of the Aggtelek-Rudabánya Mountains (in Hungarian). Földtani Kutatás 27: 49–56.

Haas J, Kovács S (2001) The Dinaric–Alpine connection — as seen from Hungary. Acta Geol Hung 44/2–3: 345–362.

Haas J, Kovács S, Krystyn L, Lein, R, (1995) Significance of Late Permian-Triassic facies zones in terrane reconstructions in the Alpine-North Pannonian domain. Tectonophysics 242: 19-40.

Haas J, Görög Á, Kovács S, Ozsvárt P, Matyók I, Pelikán P (2006) Displaced Jurassic foreslope and basin deposits of Dinaric origin in Northeast Hungary. Acta Geol Hung 49/2: 125–163.

Haas J, Budai T, Csontos L, Fodor L, Konrád Gy. (2010b) Pre-Cenozoic geological map of Hungary 1:500 000. Geological Institute of Hungary, Budapest.

Haas J, Kovács S, Gawlick H-J, Grădinaru E, Karamata S, Sudar M, Péró Cs, Mello J, Polák M, Ogorelec B, Buser S (2011a) Jurassic evolution of the tectonostratigraphic units in the Circum-Pannonian region. Jahrbuch der Geologischen Bundesanstalt 151: 281–354.

Haas J, Kovács S, Pelikán P, Kövér S, Görög Á, Ozsvárt P, Józsa S, Németh N (2011b) Remnants of the accretionary complex of the Neotethys Ocean in Northern Hungary. Földtani Közlöny 141/2: 167-196. (in Hungarian with English abstract)

Haas J, Pelikán P, Görög Á, Józsa S, Ozsvárt P (2013) Stratigraphy, facies and geodynamic setting of Jurassic formations in the Bükk Mountains, North Hungary: its relation with the other areas of the Neotethyan realm. Geol Mag 150: 18–49.

Haas J, Budai T, Csontos L, Fodor L, Konrád Gy, Koroknai B (2014) Geology to the pre-Cenozoic basement of Hungary. Explanatory notes of the “Pre-Cenozoic geological map of Hungary” (1: 500 000). Geological and Geophysical Institute of Hungary, Budapest, pp 73.

Haas J, Budai T, Dunkl I, Farics É, Józsa S, Kövér Sz, Götz AE, Piros O, Szeitz P (2017) The Budaörs-1 well revisited: Contributions to the Triassic stratigraphy, sedimentology, and magmatism of the southwestern part of the Buda Hills. Central European Geology, DOI: 10.1556/24.60.2017.008

Handy MR, Schmid SM, Bousque R, Kissling E, Bernoulli D. (2010) Reconciling plate-tectonic reconstructions of Alpine Tethys with the geological–geophysical record of spreading and subduction in the Alps. Earth Sci Rev 102: 121–158.

Héja G, Kövér Sz, Csillag G, Németh A, Fodor L (2018) Evidences for pre-orogenic passive-margin extension in a Cretaceous fold-and-thrust belt on the basis of combined seismic and field data (western Transdanubian Range, Hungary). Int J. Earth Sci. accepted

Ivan P (2002) Relics of the Meliata Ocean crust: geodynamic implications of mineralogical, petrological and geochemical proxies. Geol Carpath 53/4: 245-256.

Janák M, Plašienka D, Frey M, Cosca M, Schmidt ST, Lupták B, Méres Š (2001): Cretaceous evolution of a metamorphic core complex, the Veporic unit, Western Carpathians (Slovakia): P–T conditions and in situ 40Ar/39Ar UV laser probe dating of metapelites. J Met Geol 19: 197-216.

Kázmér M, Kovács S (1985) Permian-Paleogene Paleogeography along the Eastern part of the Insubric-Periadriatic Lineament system: Evidence for continental escape of the Bakony-Drauzug Unit. Acta Geol Hung 28: 71–84.

Kiss G, Molnár F, Palinkaš LA, Kovács S, Hrvatović H (2012) Correlation of Triassic advanced rifting related Neotethyan submarine basaltic volcanism of the Darnó Unit (NE Hungary) with some Dinaridic and Hellenidic occurrences on the basis of volcanological, fluid-rock interaction and geochemical characteristics. Int J Earth Sci 101/6: 1503—1521.

Klötzli U, Klötzli E, Günes Z, Košler J (2009): External accuracy of laser ablation U-Pb zircon dating: results from a test using five different reference zircons. Geostandards and Geoanalytical Research, 33/1: 5-15.

Kohút M, Hofmann M, Havrila M, Linnenmann U (2017) Tracking an upper limit of the "Carnian Crisis" and/or Carnian stage in the Western Carpathians (Slovakia). Int J Earth Sci. https://doi.org/10.1007/s00531-017-1491-8

Kovács S (1988) Olistostromes and other deposits connected to subaqueous mass-gravity transport in the North Hungarian Paleo–Mesozoic. Acta Geol Hung 31/3–4: 265–287.

Kovács S (2010) Type section of the Triassic Bódvalenke Limestone Formation (Rudabánya Hills, NE Hungary) - the northwesternmost occurrence of a Neotethyan deep water facies. Cent Eur Geol 53/1: 121-133.

Kovács S, Less Gy, Piros O, Réti Zs, Róth L (1989) Triassic formations of the Aggtelek-Rudabánya Mts. (Northeastern Hungary). Acta Geol Hung 32: 31–63.

Kovács S, Haas J, Ozsvárt P, Palinkaš LA, Kiss G, Molnár F, Józsa S, Kövér Sz (2010) Re-evaluation of the Mesozoic complexes of Darnó Hill (NE Hungary) and comparisons with Neotethyan accretionary complexes of the Dinarides and Hellenides — preliminary data. Cent Eur Geol 53/2–3: 205–231.

Kovács S, Sudar M, Gradinaru E, Gawlick H-J, Karamata S, Haas J, et al. (2011) Triassic Evolution of the Tectonostratigraphic Units of the Circum-Pannonian Region. Jahrbuch der Geologischen Bundesanstalt 151:201-228.

Kövér Sz, Fodor L, Judik K, Németh T, Balogh K, Kovács S (2009a) Deformation history and nappe stacking in Rudabánya Hills (Inner Western Carpathians) unravelled by structural geological, metamorphic petrological and geochronological studies. Geodin Acta 22: 3–29.

Kövér Sz, Haas J, Ozsvárt P, Görög Á, Götz AE, Józsa S (2009b) Lithofacies and age data of Jurassic foreslope and basin sediments of Rudabánya Hills (NE Hungary) and their tectonic interpretation. Geol Carpath 60/5: 351-379.

Kozur H (1991) The evolution of the Meliata-Hallstatt ocean and its significance for the early evolution of the Eastern Alps and Western Carpathians. — Palaegeography, Palaeoclimatology, Palaeoecology 87/1–4, 109–135.

Kozur H, Mock R (1985) Erster Nachweis von Jura in der Meliata-Einheit der südlichen Westkarpaten. Geol Paläont Mitt Innsbruck, 13/10: 223-238.

Kozur H, Mock R (1997) New palaeographic and tectonic interpretations in the Slovakian Carpathians and their implications for correlation with the Easten Alps and other parts of the Western Tethys. Part II: Inner Western Carpathians. Mineralia Slovaca, 29/3: 164–209.

Kozur H, Mock R, Ožvoldová L (1996) New biostratigraphic results in the Meliaticum in its type area around Meliata village (Slovakia) and their tectonic and paleogeographic significance. Geol Paläont Mitt Innsbruck 21: 89-121.

Lačný A, Plašienka D, Vojtko R (2016) Structural evolution of the Turňa Unit constrained by fold and cleavage analyses and its consequences for the regional tectonic models of the Western Carpathians. Geol Carpath 67/2:177-193.

Langone A, Zanetti A, Daczko NR, Piazolo S, Tiepolo M, Mazzucchelli M (2018) Zircon U‐ Pb Dating of a Lower Crustal Shear Zone: A Case Study From the Northern Sector of the Ivrea‐ Verbano Zone (Val Cannobina, Italy). Tectonics 37/1: 322-342

Less Gy (2000) Polyphase evolution of the structure of the Aggtelek–Rudabánya Mountains (NE Hungary), the southernmost element of the Inner Western Carpathians – a review. Slovak Geol Mag 6/2-3: 260–268.

Less Gy, Mello J (eds.) (2004) Geological map of the Gemer-Bükk area 1:100000. Geol Inst of Hungary, Budapest.

Lexa O, Schulmann K, Jezek J (2003) Cretaceous collision and indentation in the Western Carpathians: View based on structural analysis and numerical modelling. Tectonics 22 Art. No. 1066.

Ludwig KR (2003) Isoplot/Ex 3.00: A geochronological toolkit for Microsoft Excel. Berkeley Geochronology Center Special Publication 4, pp 70.

Maffione M, Thieulot C, van Hinsbergen DJJ, Morris A, Plumper O, Spakman W (2015), Dynamics of intra-oceanic subduction initiation. 1: Oceanic detachment fault inversion and the formation of forearc ophiolites, Geochem Geophys Geosyst, doi:10.1002/2015GC005746.

Maluski H, Rajlich P, Matte P (1993) 40Ar/39Ar dating of the Inner Carpathians Variscan basement and Alpine mylonitic overprint. Tectonophysics 223: 313-337.

Majoros P (2008) Az Aggtelek–Rudabányai- és Bükk–hegység jura koru vulkanitjainak cirkonmorfológiai vizsgálata. MSc thesis, Department of Mineralogy and Petrology, University of Miskolc. In Hungarian

Máthé Z, Szakmány Gy (1990) The genetics (formation) of rhyolite occurring in the Rudabánya Mts. (Northeastern Hungary). Acta Miner-Petrogr, Szeged 30: 81–92.

McDonough WF, Sun SS (1995) Composition of the Earth. Chemical Geology 120: 223-253.

Mello J (1979) Meliata sequence in the Turna tectonic window. Geol Práce 72: 61-76.

Mello J, Elečko M, Pristaš J, Reichwalder P, Snopko D, Vass D, Vozárová A (1996) Geological map of the Slovenský Kras Mts., 1:50000. Geol. Survey of the Slovak Republic, Bratislava.

Mello, J., Reichwalder, P., Vozárová, A. (1998). Bôrka nappe: high-pressure relic from the subduction-accretion prism of the Meliata ocean (Inner Western Carpathians, Slovakia). Slovak Geological Magazine, 4, 261–273.

Méres Š., Ivan P., Konečný P., Aubrecht R., Sýkora M., Plašienka D. & Reichwalder P., 2013: Two monazite ages from the accretionary prism mélange of the Meliata Ocean (Bôrka Nappe, Meliatic Superunit, Western Carpathians). In Broska I. & Tomašových A. (eds): Geological evolution of the Western Carpathians: new ideas in the field of inter-regional correlations. Abstract Book, Internat. Conference GEEWEC 2013, Smolenice, Slovak Republic, October 16–19, 2013. Geol. Inst. SAS, Bratislava, 58–59.

Mock R, Sykora M, Aubrecht R, Ozvoldová L, Kronome B, Reichwalder P, Jablonsky J (1998) Petrology and stratigraphy of the Meliaticum near the Meliata and Jaklovce Villages, Slovakia. Slovak Geol Mag 4: 223–260.

Mundil R, Brack P, Meier M, Rieber H, Oberli F (1996) High resolution U-Pb dating of Middle Triassic volcaniclastics: Time-scale calibration and verification of tuning parameters for carbonate sedimentation. Earth and Planetary Science Letters 141: 137-151

Németh K, Budai T (2009) Diatremes cut through the Triassic carbonate platforms in the Dolomites? Evidences from and around the Latemar, Northern Italy. Episodes. 32/2: 74-83.

Neubauer F, Liu X, Borojevic Sostaric S, Friedl G, Heberer B, Dong Y (2014) U-Pb zircon ages of Middle-Upper Triassic magmatism in Southern Alps and NW Dinarides: implications for the Southeast Mediterranean tectonics. Proceedings of the XXth Congress of the CBGA. Tirana, Albania, Buletini I Shkencave Gjeologjike 2: 217.

Ortner H (2017) Geometry of growth strata in wrench dominated transpression: 3D model of the Upper Jurassic Trattberg rise, Northern Calcareous Alps, Austria Geophys. Res. Abstracts 19. EGU 2017 T9222.

Pálfy J, Parrish RR, David K, Vörös A (2003) Mid-Triassic integrated U–Pb geochronology and ammonoid biochronology from the Balaton Highland (Hungary). J Geol Soc London, 160: 271–284.

Pamič J, Lovrič A (1980) Geological and isotope ages of the rift magmatien of the Mesozoic Wilson cycle in the Dinarides. Symposium de Géologie Régionale et Paléontologie – Institut de Géologie Régional et de Paléontologie, Faculté des Mines et de Geologie Universite de Belgrade. 251-274

Pelikán P, Less Gy, Kovács S, Pentelényi L, Sásdi L. (2005) Geology of the Bükk Mountains. Explanatory Book to the Geological Map of the Bükk Mountains (1:50000). Geological Institute of Hungary, Budapest, pp 284.

Plašienka D (1997) Cretaceous tectonochronology of the Central Western Carpathians (Slovakia). Geol Carpath 48: 99-111.

Plašienka D, Grecula P, Putiš M, Hovorka D, Kováč M (1997). Evolution and structure of the Western Carpathians: an overview. In: Grecula P, Hovorka D, Putiš M (eds.): Geological Evolution of the Western Carpathians. Mineralica Slovaca Monograph, Bratislava, 1–24.

Plašienka D (1998) Paleotectonic evolution of the Central Western Carpathians during the Jurassic and Cretaceous. In: Rakús M (ed.): Geodynamic development of the Western Carpathians. Geol Survey of Slovak Republic, Bratislava, 107–130.

Pleničar M, Ogorelec B, Novak M (2009) The Geology of Slovenia. Geoloski zavod Slovenije, Ljubljana pp 612.

Schmid SM, Bernoulli D, Fügenschuh B, Matenco L, Schefer S, Schuster R, Tischler M, Ustaszewski K (2008) The Alpine-Carpathian-Dinaric orogenic system: correlation and evolution of tectonic units. Swiss J Geosci 101: 139-183.

Schmidt T, Blau J, Kázmér M (1991) Large-scale displacement of the Drauzug and the Transdanubian Mountains in early Alpine history: evidence from Permo-Mesozoic facies belts. Tectonophysics, 200: 213-232.

Sláma J, Košler J, Condon DJ, Crowley JL, Gerdes A, Hanchar JM, Horstwood MSA, Morris GA, Nasdala B, Turbett MN, Whitehouse MJ (2008) Plešovice, a new natural reference material for U–Pb and Hf isotopic analysis. Chem Geol 249: 1–35.

Sylvester PJ, Ghaderi M (1997). Trace element analysis of scheelite by excimer laser ablation-inductively coupled plasma mass spectrometry (ELA-ICPMS) using a synthetic silicate glass standard. Chemical Geology 141: 49–65.

Stacey JS, Kramers JD (1975) Approximation of terrestrial lead isotope evolution by a two-stage model. Earth and Planetary Science Letters 26: 207–221.

Stampfli GM, Borel GD (2002) A plate tectonic model for the Paleozoic and Mesozoic constrained by dynamic plate boundaries and restored synthetic oceanic isochrons. Earth and Plan Sci Letters, 196/1-2: 17-33

Stüwe K, Schuster R (2010) Initiation of subduction in the Alps: Continent or ocean? Geology 38: 175–178.

Sun SS, McDonough WF (1989) Chemical and isotopic systematics of oceanic basalts: implications for mantle composition and processes. Geol Soc London Spec Pub 42/1: 313-345.

Velledits F (2006) Evolution of the Bükk Mountains (NE Hungary) during the Middle–Late Triassic asymmetric rifting of the Vardar-Meliata branch of the Neotethys Ocean. Int J Earth Sci 95/3: 395-412.

Vörös A (2010) Late Anisian Ammonoidea from Szár-hegy (Rudabánya Mts); a Dinaric-type fauna from North Hungary. Fragmenta Palaeontologica Hungarica 28: 1–20.

Wolff R, Dunkl I, Kiesselbach G, Wemmer K, Siegesmund S (2012) Thermochronological constraints on the multiphase exhumation history of the Ivrea‐ Verbano Zone of the Southern Alps. Tectonophysics 579: 104–117.

Wotzlaw JF, Brack P, Storck JC (20187) High-resolution stratigraphy and zircon U–Pb geochronology of the Middle Triassic Buchenstein Formation (Dolomites, northern Italy): precession-forcing of hemipelagic carbonate sedimentation and calibration of the Anisian–Ladinian boundary interval. J Geol Soc 175: 71-85

Zelenka T, Baksa Cs, Balla Z, Földessy J, Földessy-Járányi K (1983) The role of the Darnó Line in the basement structure of Northeastern Hungary. Geologicky Zbornik — Geol Carpath 34/1: 53–69.

Figure captions

Fig. a) Main structural units of the Northern Pannonian Basin and surrounding areas (modified after Schmid et al. 2008). The areas of interest and location of more detailed maps are indicated by boxes. RW – Rechnitz window, TW – Tauern window **b)** Structural sketch of the Jasov area (Less and Mello 2004) and nappe superposition of the Inner Western Carpathians. Sample Mel was taken from a rhyolite block of the Meliata mélange nappe. **c)** Structural sketch map of the Telekesoldal area, and nappe superposition of the Rudabánya Hills (Kövér et al. 2009b). Samples To-1-5 were taken from different rhyolite blocks of the Telekesoldal mélange nappe. **d)** Structural sketch map and nappe superposition of the Bükk Mts (modified from Less and Mello 2004 with the nappe concept of Balla 1983 and Csontos 1988). Sample BüMel was taken from a rhyolite block of the Mónosbél mélange nappe. Location is indicated by blue circle. **e)** Geological map of the Lajse area, Slovenia (after Grad et al. 1974). Samples Slo-1 and -2 are indicated by orange diamonds.

Fig. 1 Late Jurassic paleogeographic reconstruction of the Vardar oceanic embayment (Neotethys Ocean) after Schmid et al. 2008. Blue signs indicate the possible paleogeographic locations for investigated Jurassic mélange nappes with redeposited rhyolite and andesite clasts. (To – Telekesoldal nappe, Mel – Meliata nappe, BüMel – mélange nappe of the Bükk Mts.: Mónosbél nappe). Paleogeographic location of in-situ Late Triassic acidic effusive rocsk is indicated. (Slo-Slovenian Trough).

Fig. 3 Cathodoluminescence (CL) and back-scattered electron (BSE) images of the zircon crystals from sample To-1(1) of the TO mélange nappe. Measured spots and tracks are indicated. U-Pb concordia and Tera-Wasserburg plots of the adjacent zircon samples. Plot 1: 1-b-a track, 1-c-3 track A, 1-e-6 track; Plot 2: 1-b-1 track, 1-a-4 spot B

Fig. 4 Cathodoluminescence (CL) and back-scattered electron (BSE) images of the zircon crystals from sample To-1(2) and To-1(3) of the TO mélange nappe. Measured spots and tracks are indicated. Tera-Wasserburg plot of the adjacent zircon samples is presented.

Fig. 5 Cathodoluminescence (CL) and back-scattered electron (BSE) images of the zircon crystals from sample To-3(8) and To-2(7) of the TO mélange nappe. Measured spots and tracks are indicated. Tera-Wasserburg plot of the adjacent zircon samples is presented.

Fig. 6 Cathodoluminescence (CL) and back-scattered electron (BSE) images of the zircon crystals from sample To-5(4) of the TO mélange nappe. Measured spots and tracks are indicated. Tera-Wasserburg plot of the adjacent zircon samples is presented.

Fig. 7 Cathodoluminescence (CL) and back-scattered electron (BSE) images of the zircon crystals from sample BüMel/11 of the Mónosbél mélange nappe, Bükk Mts. Measured spots and tracks are indicated. Tera-Wasserburg plot of the adjacent zircon samples is presented.

Fig. 8 TAS diagram of the rhyolite clast and block samples from the different Middle – Upper Jurassic mélange nappes and in situ Upper Triassic samples from the Slovenian Trough. For sample locations see Fig 1.

Fig. 9 a) Chondrite normalized (McDonough, Sun 1985, Sun, McDonough 1989) REE pattern of the rhyolite clasts from different mélange nappes and in situ Upper Triassic rhyolite/tuff samples showing considerable enrichment LREE, while significantly smaller enrichment in HREE. Grey band corresponds to Rift/Continental Margin-type magma of Furnes and Dilek 2017 **b)** distribution of La/Lu numbers within the analysed rhyolite clasts and in situ Upper Triassic samples

Fig. 2 a,b) Chondrite normalized (McDonough, Sun 1985, Sun, McDonough 1989**)** trace element pattern of the rhyolite clasts from different mélange nappes and in situ Upper Triassic rhyolite/tuff samples (blue signs are for TO mélange nappe, red is for Meliata mélange, yellow is for Mónosbél mélange, Bükk Mts, while orange is for the in situ Upper Triassic samples). Grey band corresponds to Rift/Continental Margin-type magma of Furnes and Dilek 2017. **c)** Th/Yb vs Ta/Yb discrimination diagram of Gorton and Schandal 2000. Within plate volcanism is the most probable tectonic setting for rhyolite clasts from different mélange nappes and in situ Upper Triassic rhyolite/tuff samples.

Fig. 3 Radiometric ages of magmatic events in the western termination of the Neotethys Ocean. Blue signs are from present study. The typical, rift-related pietra verda-type magmatism is represented by samples from the Silvretta nappe, Dolomites and TR. Younger events are present in form of detrital zircons in the Lunz beds (WC), as dykes and diatremes in the Dolomites and as volcanic layers in the Dinarides.

Fig. 12 Paleogeographic sketch of the western termination of the Neotethys Ocean. a) Middle – Late Jurassic b) Early Cretaceous. Transparent grey represents the obducting ophiolite nappe. Deformation of the lower plate is indicated below it. Late Triassic facies zones on the continental margin (purple letters): HD Haupdolomite facies zone (lagoon), D Dachstein facies zone (platform) R Reef of the Dachstein platform, Zl Zlambach facies zone (slope), H Hallstatt facies zone (pelagic basin), Meli Meliata facies zone (ocean – continent transition). Supposed palinspastic position of the Mesozoic structural units: ADCP Adriatic-Dinaric Carbonate Platform, Bó Bódva nappe (Rudabánya Hills), Bô Bôrka nappe, Bu (Buda Hills of TR), Bü Bükk nappe, Da Darnó mélange nappe (Bükk Mts.), Dr Drauzug, Dol Dolomites, Ju Julian Alps, Mel Meliata nappe, Mó Mónosbél nappe (Bükk Mts.), Sl-T Slovenian Trough, SOM Sub-ophiolitic mélange, Sz Szarvaskő nappe (Bükk Mts.), Tn Turňa/Torna nappe (Western Carpathians), TR Transdanubian Range, To Telekesoldal nappe (Rudabánya Hills)

Table captions

Table 1 Corrected isotope ratios of the measured samples.

Table 2 Representative major element chemical compositions of rhyolite clasts from different mélange nappes and in situ Upper Triassic rhyolite/tuff samples. For sample locations see Fig 1.

Table 3 Representative trace element chemical compositions of rhyolite clasts from different mélange nappes and in situ Upper Triassic rhyolite/tuff samples. For sample locations see Fig 1.

Figure 01

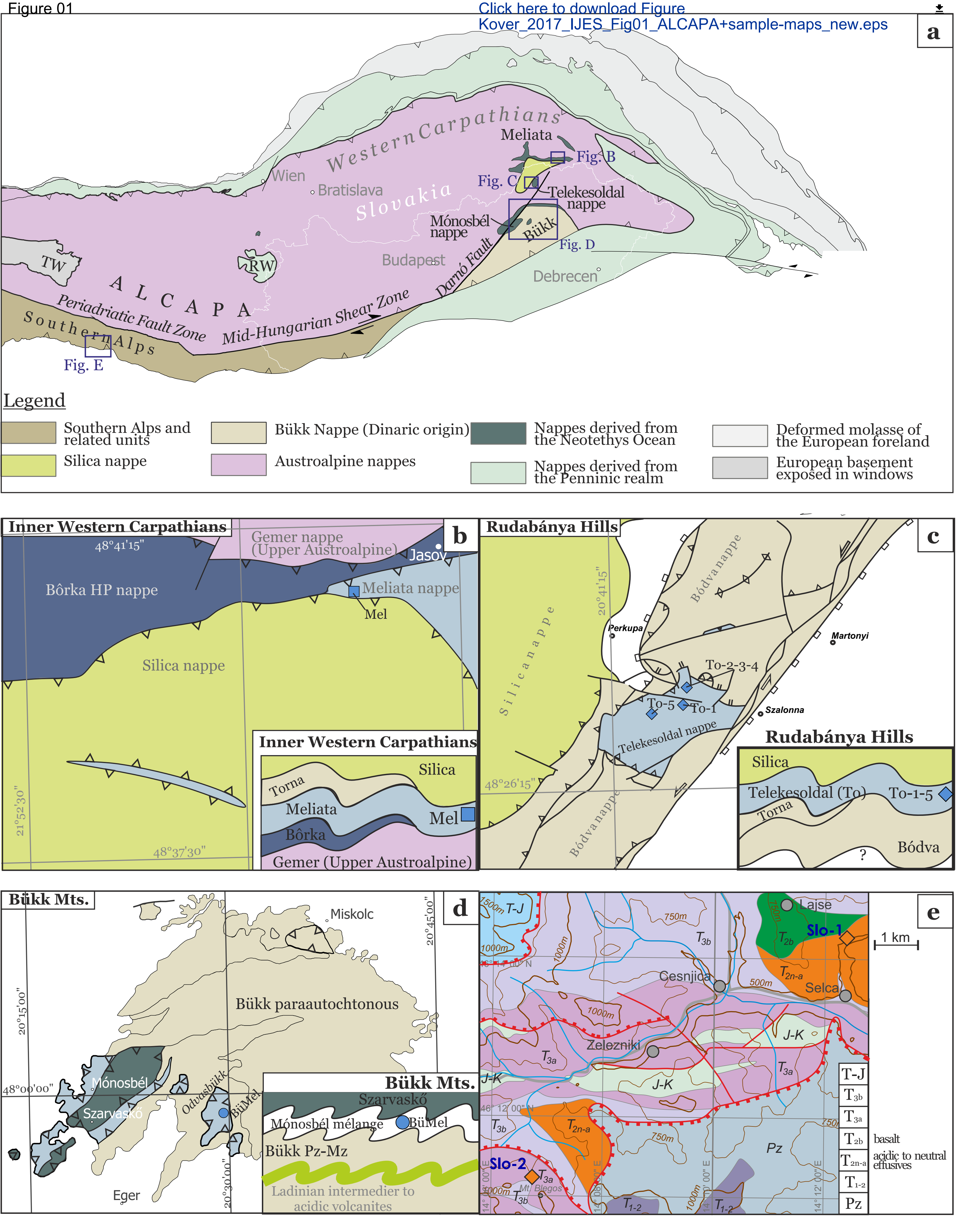
a
Western Carpathians
Meliata
Fig. B
Wien
Bratislava
Slovakia
Fig. C
Telekesoldal nappe
Mónosbél nappe
Bükk
Fig. D
TW
RW
Budapest
Debrecen
Darnó Fault
A L C A P A
Periadriatic Fault Zone
Mid-Hungarian Shear Zone
Southern Alps
Fig. E
Legend
Southern Alps and related units
Bükk Nappe (Dinaric origin)
Nappes derived from the Neotethys Ocean
Deformed molasse of the European foreland
Silica nappe
Austroalpine nappes
Nappes derived from the Penninic realm
European basement exposed in windows
b
Inner Western Carpathians
48°41'15"
Gemer nappe (Upper Austroalpine)
Jasov
Bôrka HP nappe
Meliata nappe
Mel
Silica nappe
21°52'30"
48°37'30"
Inner Western Carpathians
Silica
Torna
Meliata
Mel
Bôrka
Gemer (Upper Austroalpine)
c
Rudabánya Hills
Bódva nappe
20°41'15"
Perkupa
Martonyi
Silica nappe
To-2-3-4
To-5
To-1
Szalonna
Telekesoldal nappe
48°26'15"
Bódva nappe
Rudabánya Hills
Silica
Telekesoldal (To)
To-1-5
Torna
Bódva
?
d
Bükk Mts.
Miskolc
20°45'00"
Bükk paraautochtonous
20°15'00"
48°00'00"
Mónosbél
Szarvaskő
Odvasbükk
BüMel
Eger
20°30'00"
Bükk Mts.
Szarvaskő
Mónosbél mélange
BüMel
Bükk Pz-Mz
Ladinian intermedier to acidic volcanites
e
T-J
1500m
1000m
750m
T3b
Lajse
Slo-1
T2b
1 km
T2n-a
Cesnjica
500m
Selca
1000m
J-K
Zelezniki
T3a
J-K
J-K
T3a
46°12'00"N
T3b
T2n-a
750m
Pz
Slo-2
T3a
Mt. Blegos
T3b
T1-2
T1-2
T-J
T3b
T3a
T2b basalt
T2n-a acidic to neutral effusives
T1-2
Pz

Figure 02

Click here to download Figure Kover_2017_IJES_Fig02_paleogeography_new.eps

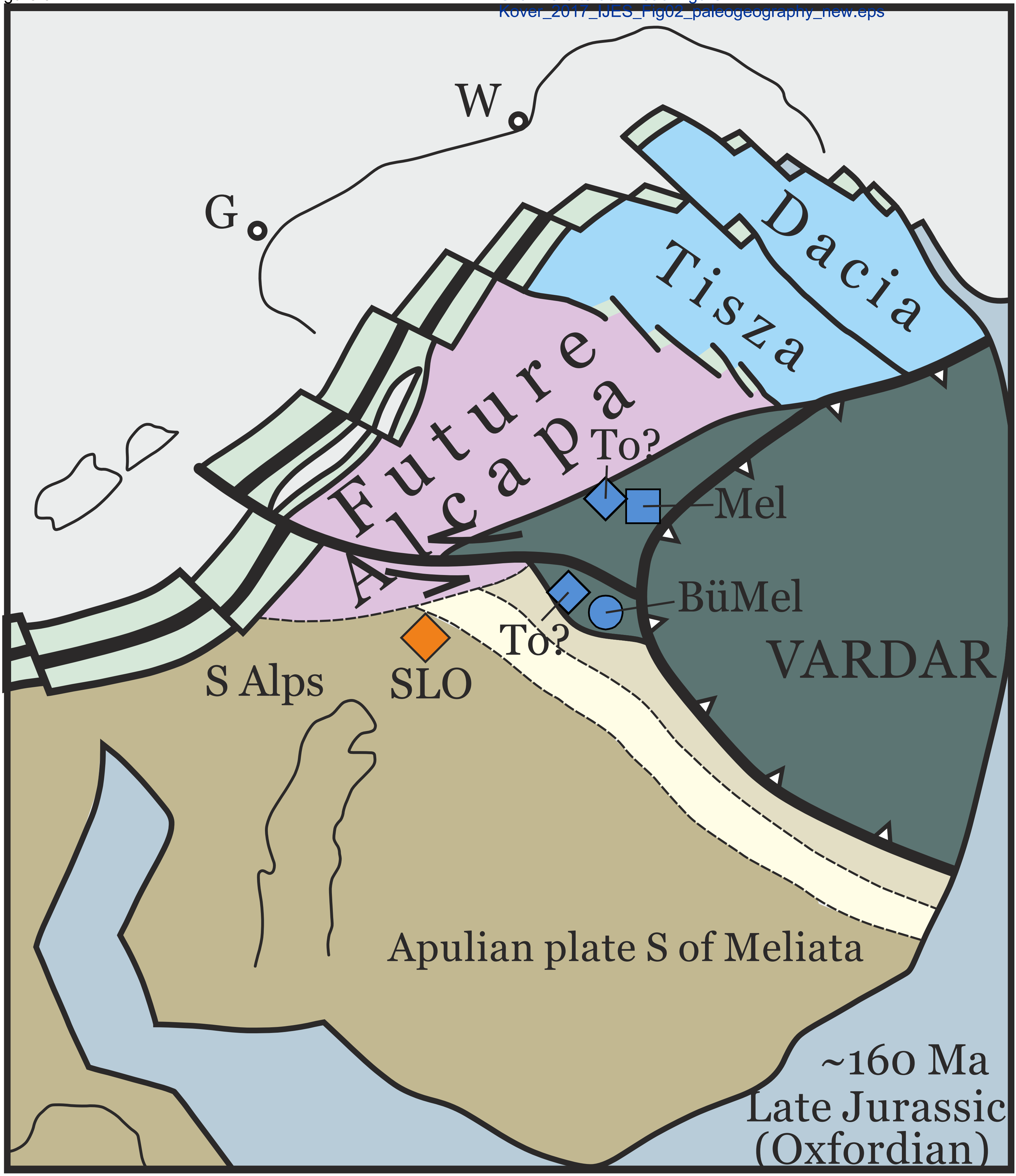

Redeposited magmatic clasts in Jurassic melange

autochtonous Late Triassic effusive rocks

Figure 03

Click here to download Figure Kover_2017_IJES_Fig03_zircon_new.tif

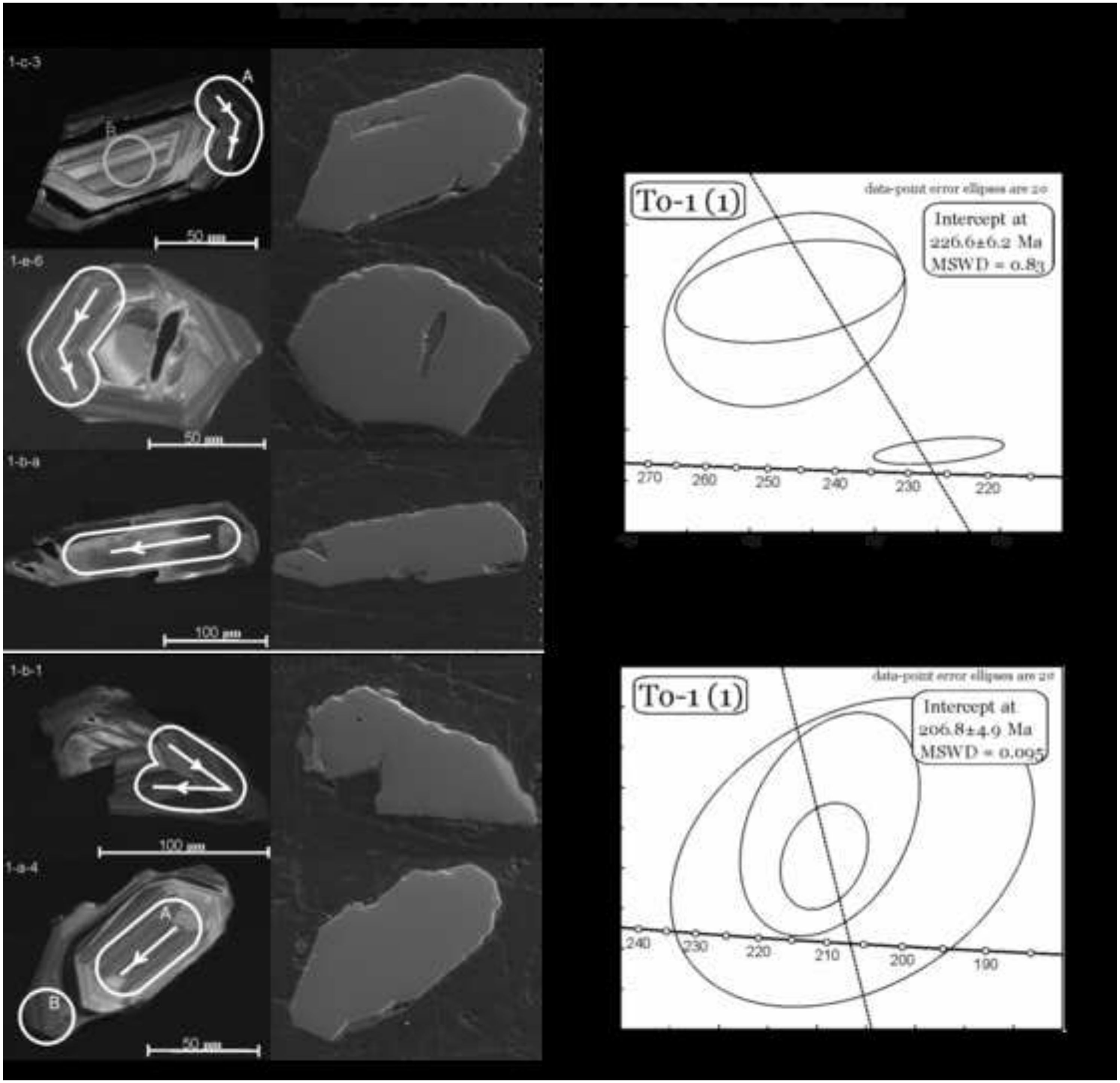

Figure 04

Click here to download Figure Kover_2017_IJES_Fig04.tif

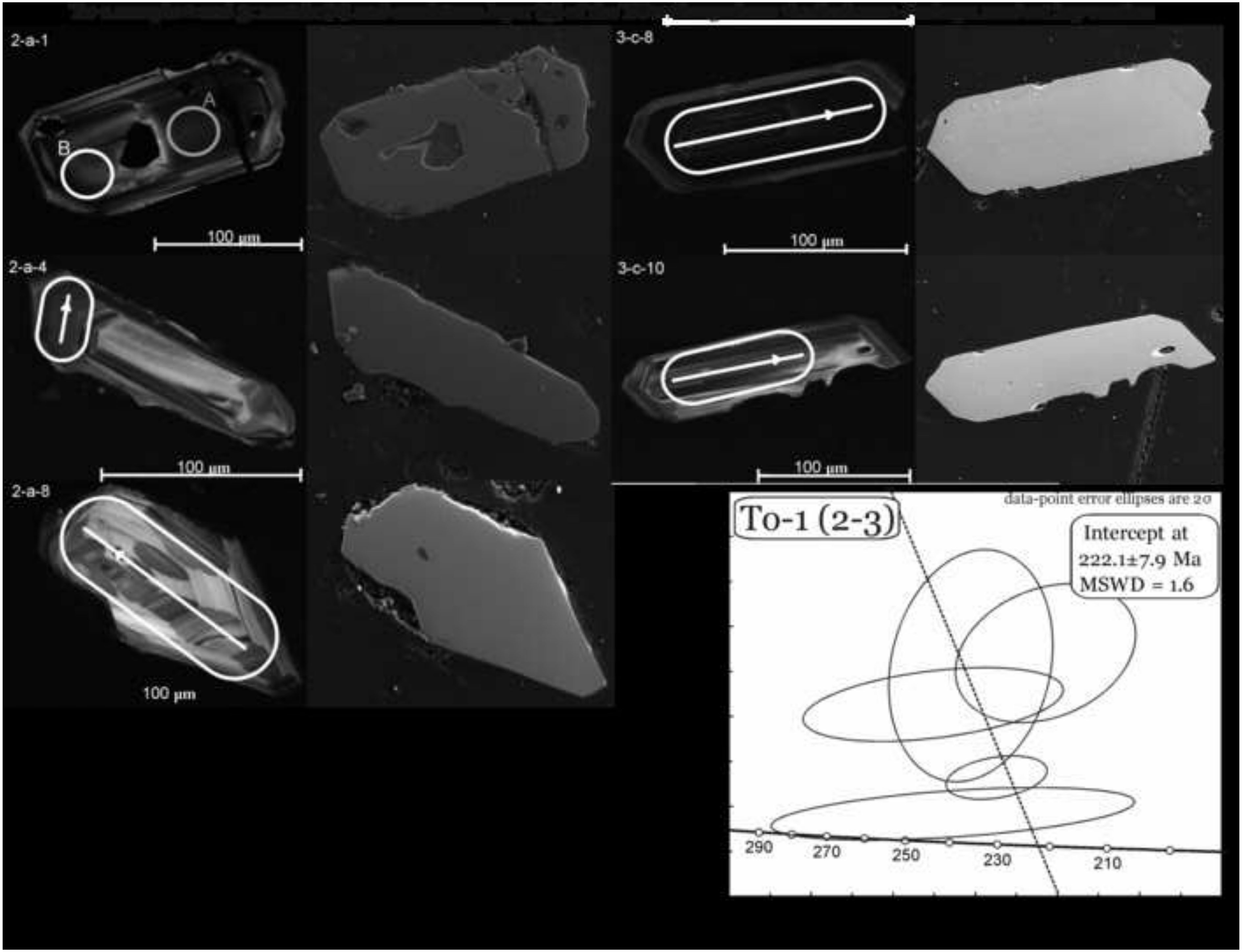

Figure 05

Click here to download Figure Kover_2017_IJES_Fig05.tif

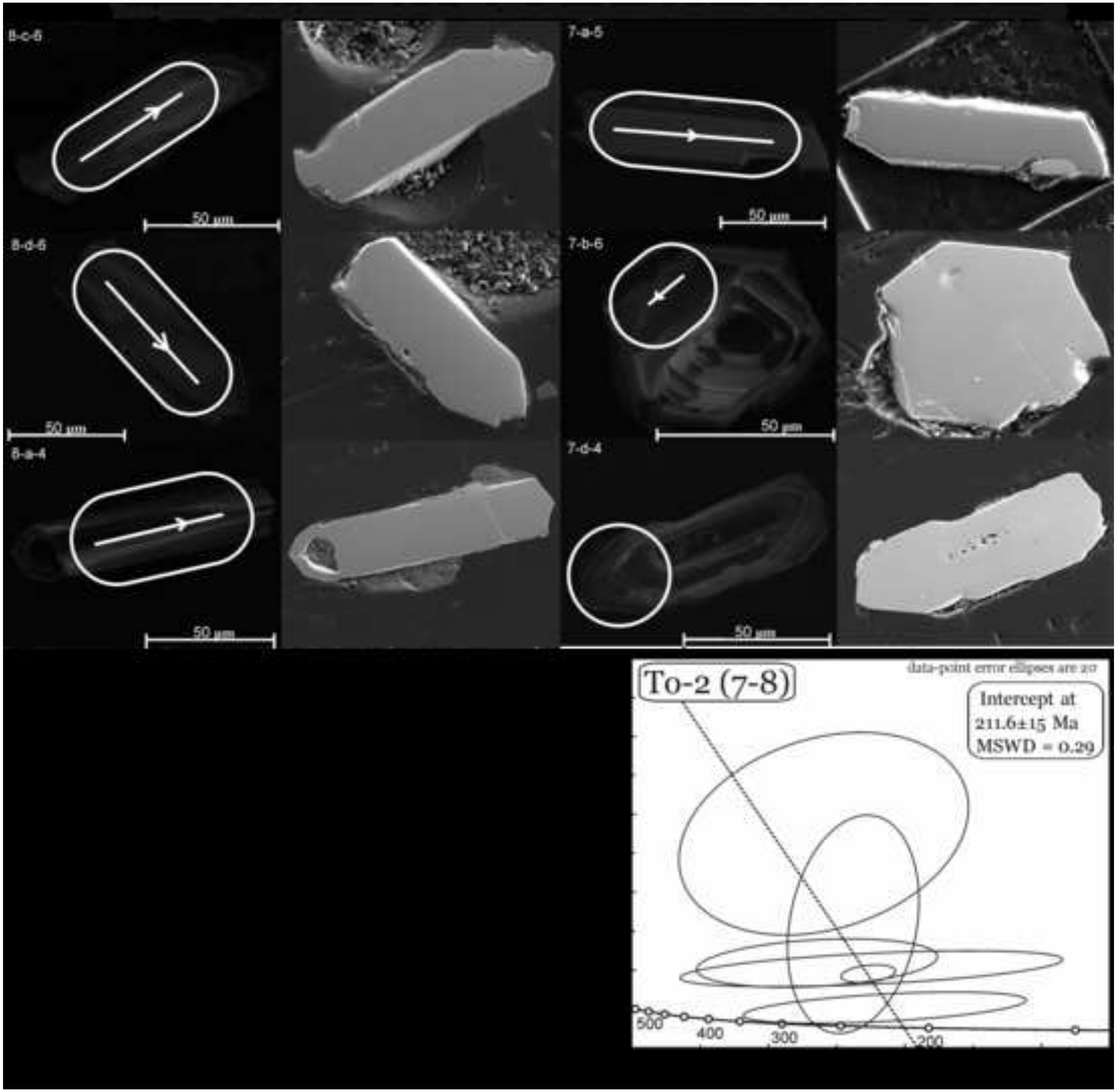

Figure 06

Click here to download Figure Kover_2017_IJES_Fig06.tif

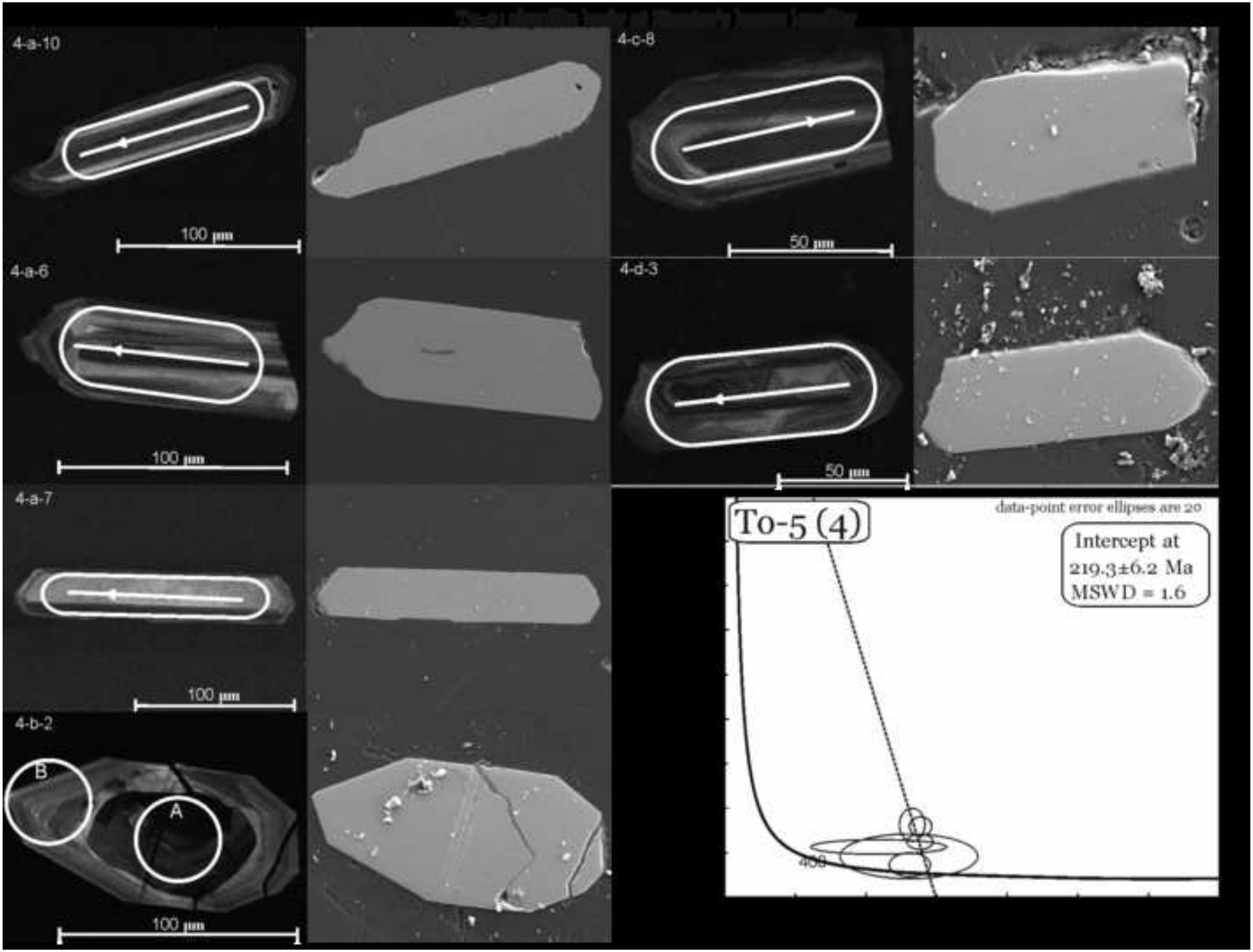

Figure 07

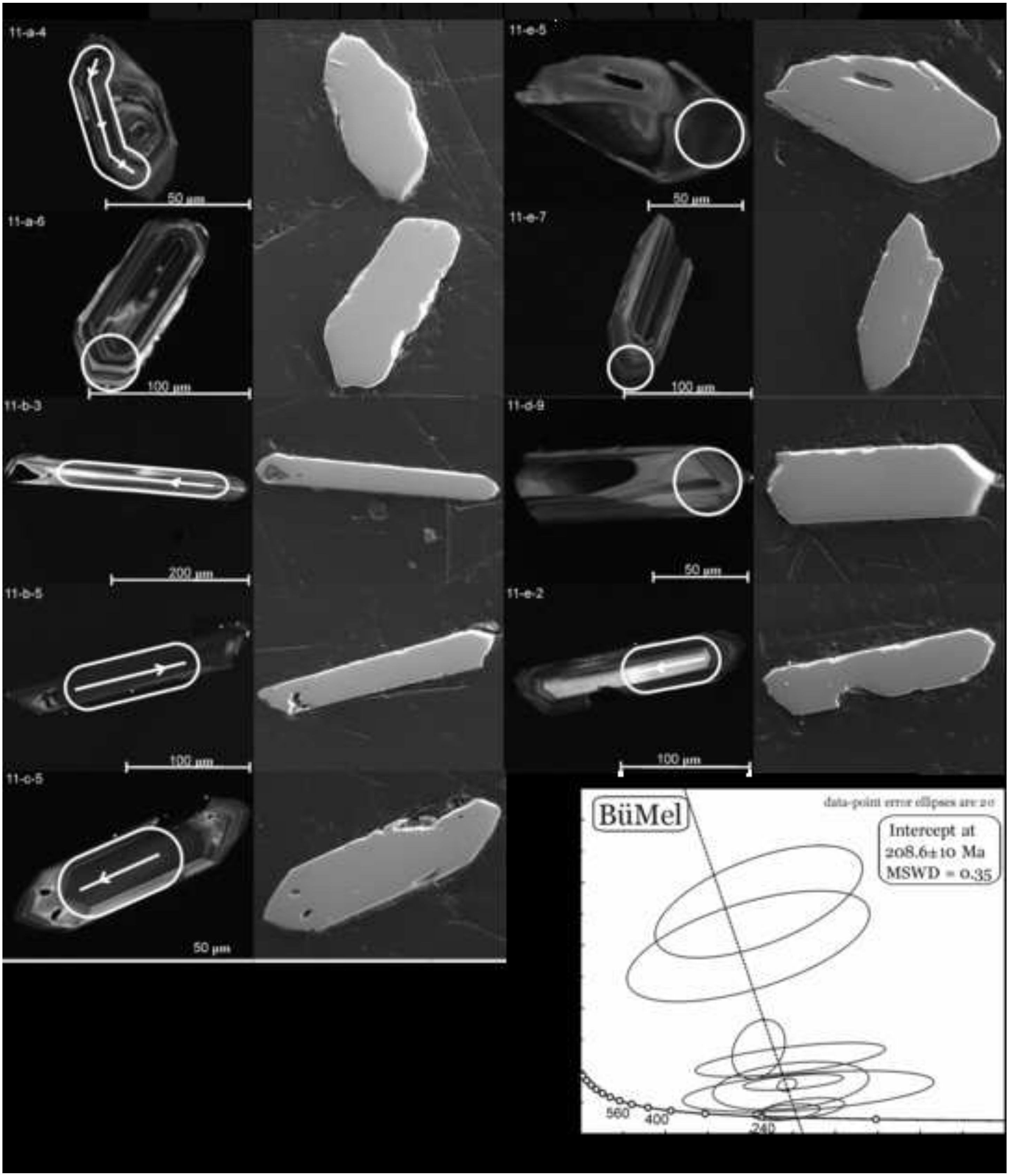
11-a-4
50 µm
11-e-5
50 µm
11-a-6
100 µm
11-e-7
100 µm
11-b-3
200 µm
11-d-9
50 µm
11-b-5
100 µm
11-e-2
100 µm
11-c-5
50 µm
BüMel
data-point error ellipses are 2σ
Intercept at
208.6±10 Ma
MSWD = 0.35
560
400
240

Figure 08

Click here to download Figure Kover_2017_IJES_Fig08_TAS_new.eps

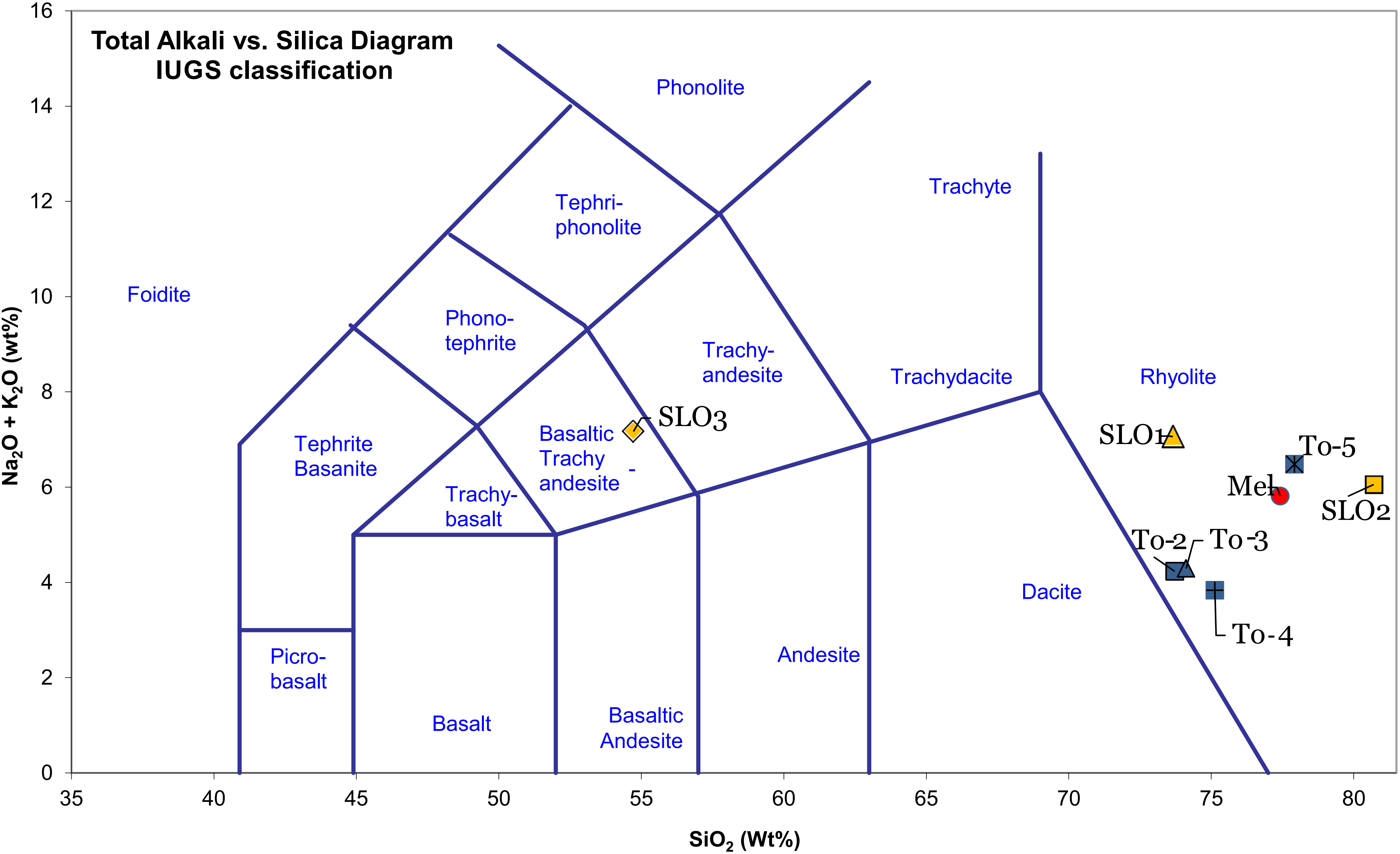

Figure 09

Click here to download Figure Kover_2017_IJES_Fig09_REE_new.eps

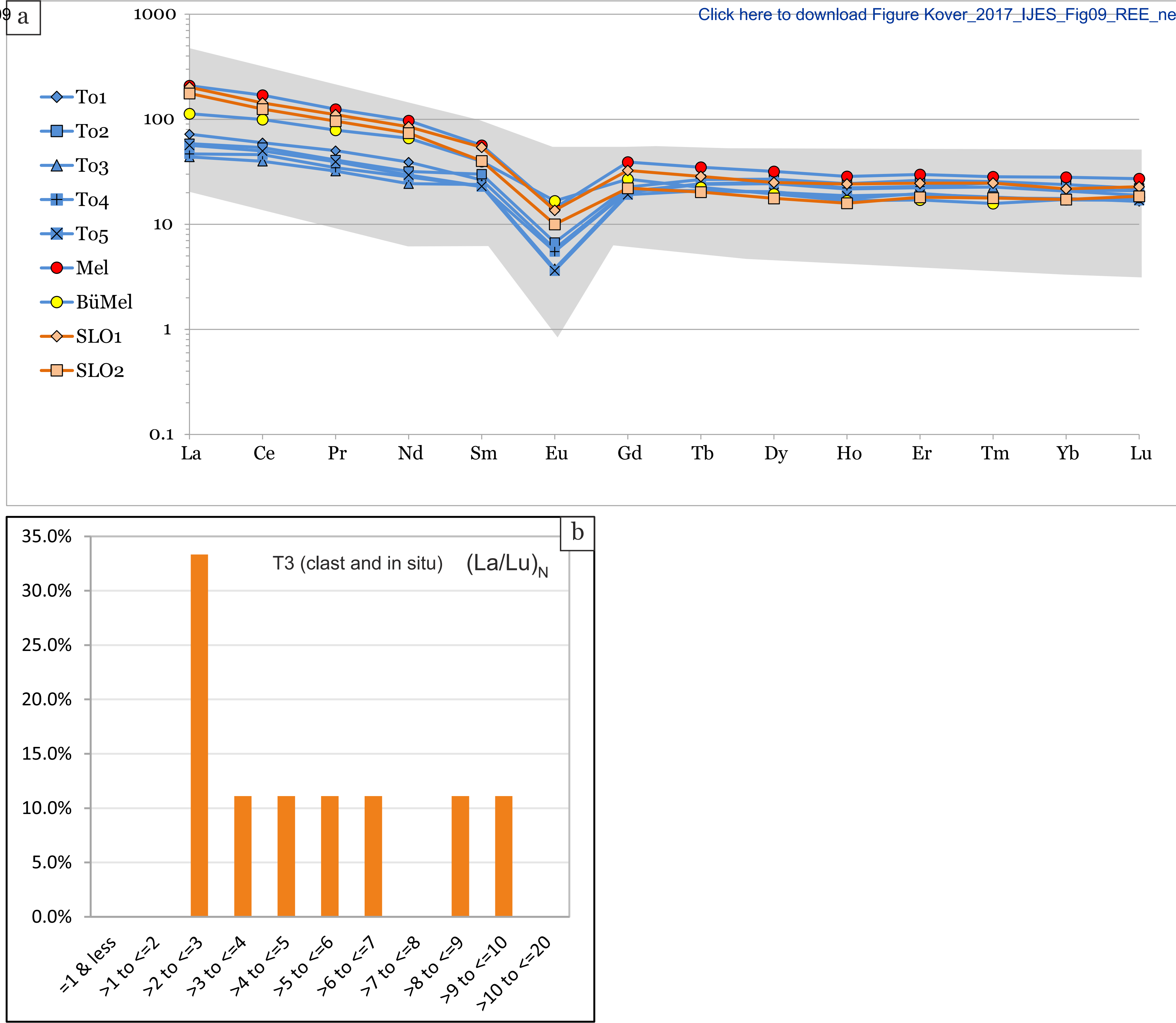

Figure 10

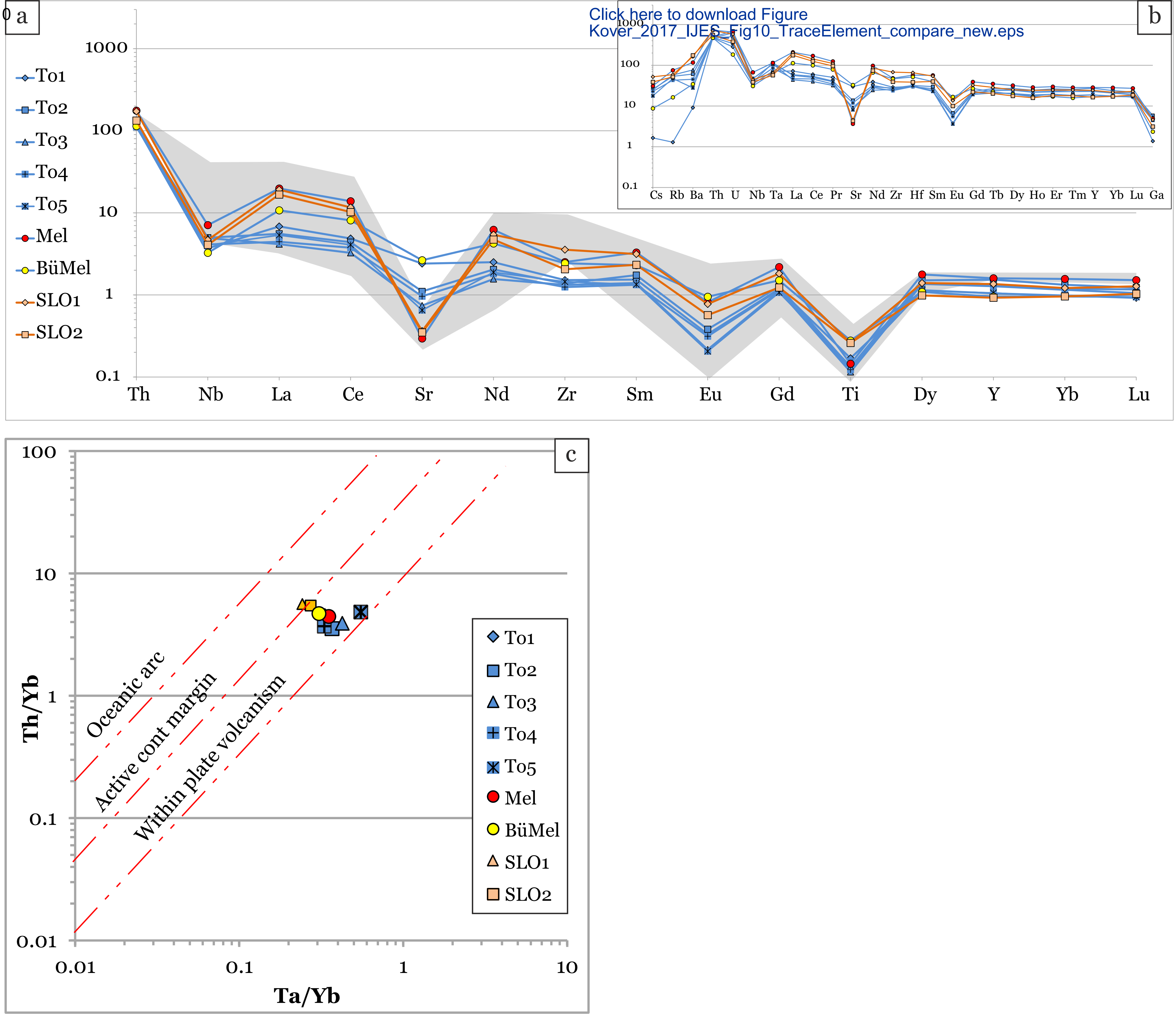
a
To1
To2
To3
To4
To5
Mel
BüMel
SLO1
SLO2
1000
100
10
1
0.1
Th Nb La Ce Sr Nd Zr Sm Eu Gd Ti Dy Y Yb Lu
b
1000
100
10
1
0.1
Cs Rb Ba Th U Nb Ta La Ce Pr Sr Nd Zr Hf Sm Eu Gd Tb Dy Ho Er Tm Y Yb Lu Ga
c
Th/Yb
Ta/Yb
100
10
1
0.1
0.01
0.01
0.1
1
10
Oceanic arc
Active cont margin
Within plate volcanism
To1
To2
To3
To4
To5
Mel
BüMel
SLO1
SLO2

Figure 11

Click here to download Figure Kover_2017_IJES_Fig11_ages_new.eps

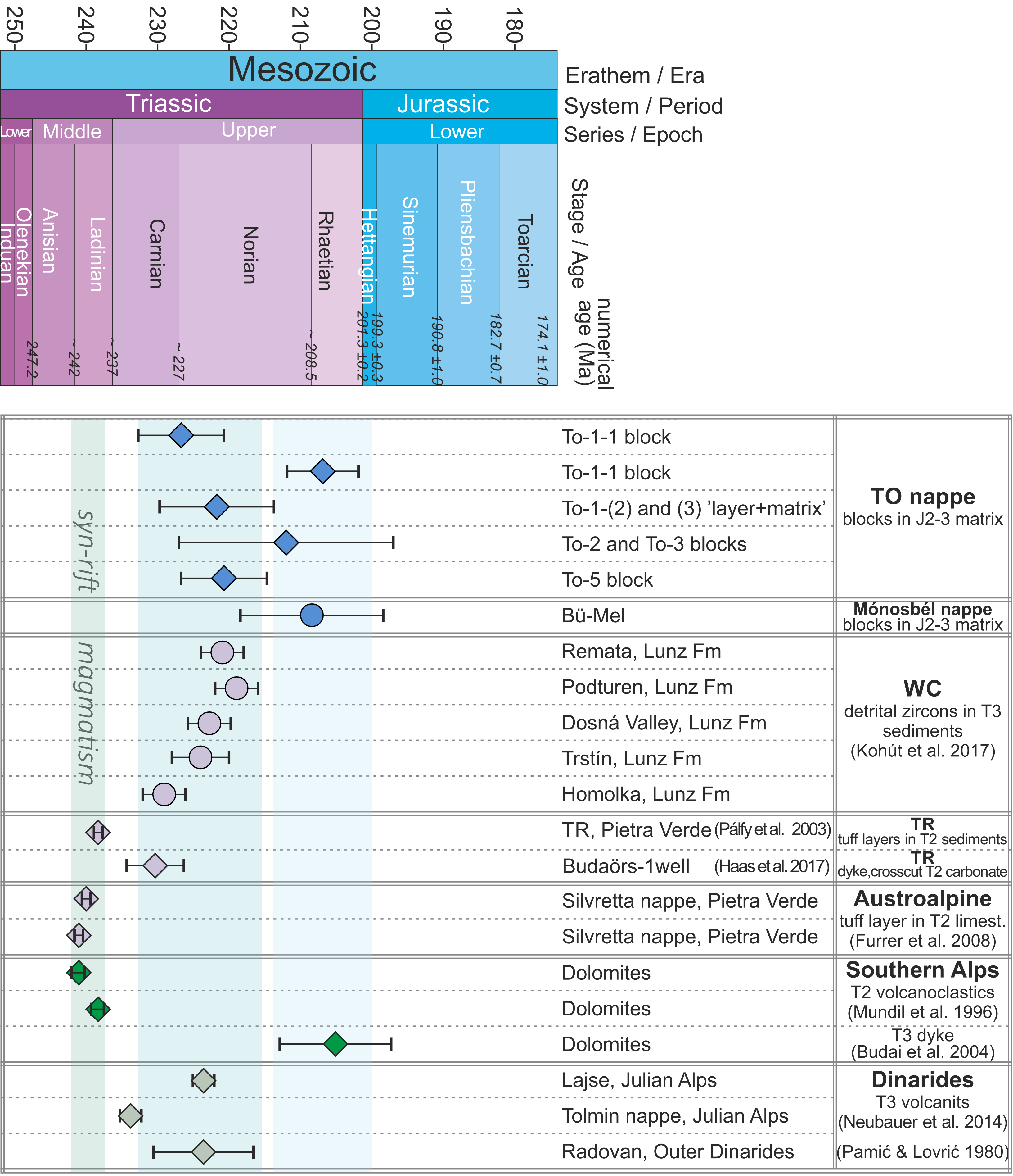

Figure 12

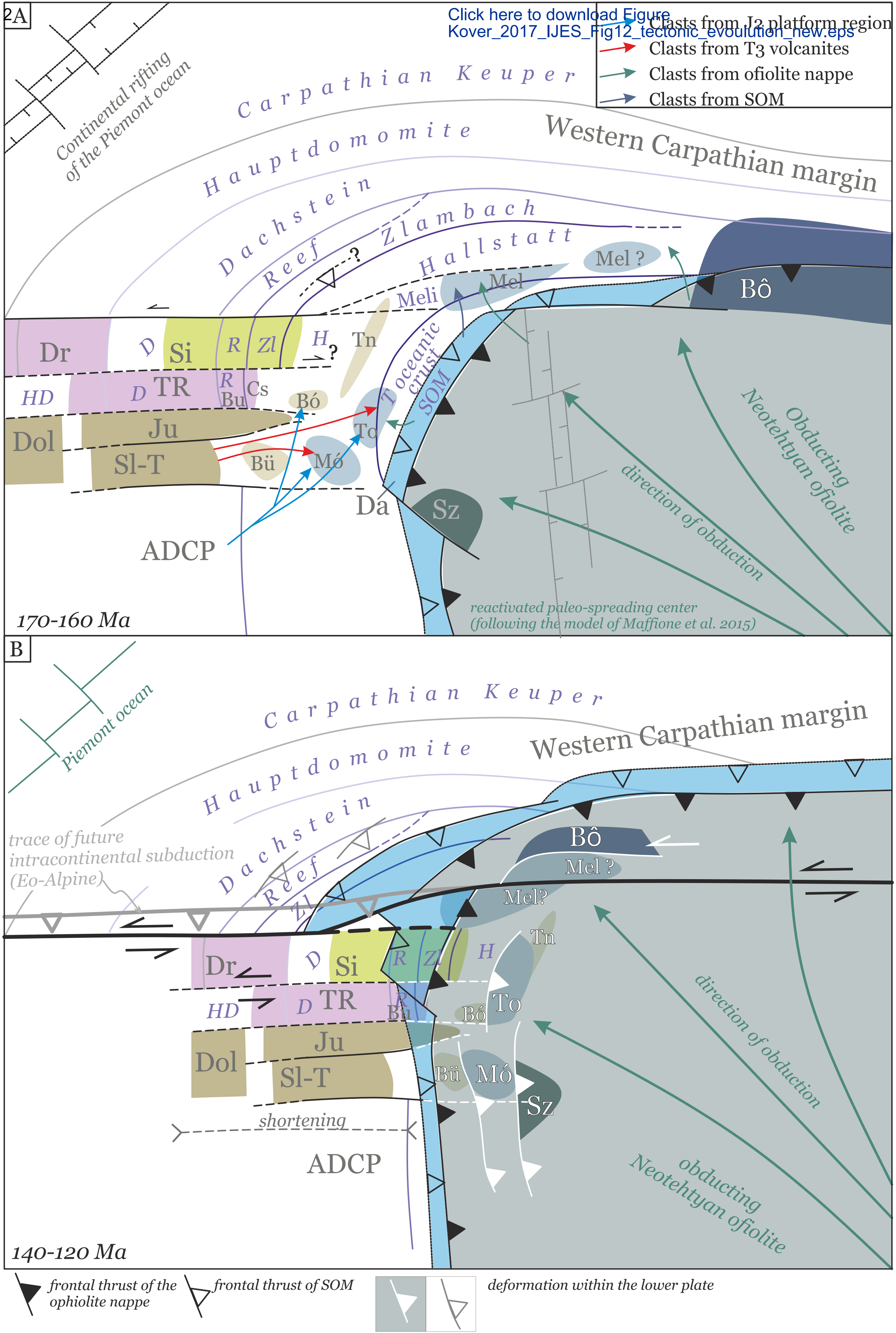
A
Clasts from J2 platform region
Clasts from T3 volcanites
Clasts from ofiolite nappe
Clasts from SOM
Continental rifting of the Piemont ocean
Carpathian Keuper
Hauptdomomite
Western Carpathian margin
Dachstein
Reef
Zlambach
Hallstatt
Mel ?
Mel
Meli
Bô
Dr
D
Si
R
Zl
H
Tn
HD
TR
Bu
Cs
Bó
T oceanic crust
SOM
Dol
Ju
Sl-T
Bü
Mó
To
Dá
Sz
ADCP
Obducting Neotethyan ofiolite
direction of obduction
reactivated paleo-spreading center (following the model of Maffione et al. 2015)
170-160 Ma
B
Piemont ocean
Carpathian Keuper
Hauptdomomite
Western Carpathian margin
Dachstein
Reef
trace of future intracontinental subduction (Eo-Alpine)
Bô
Mel ?
Mel?
Dr
D
Si
R
Zl
H
Tn
HD
TR
Bu
Bó
To
Dol
Ju
Sl-T
Bü
Mó
Sz
shortening
ADCP
direction of obduction
obducting Neotethyan ofiolite
140-120 Ma
frontal thrust of the ophiolite nappe
frontal thrust of SOM
deformation within the lower plate

Table 01

Plot	Sample number	Zircon indivicual number	Part of crystal	CL character	207Pb235U	2 σ
Fig. 03A	To-1(1)	100301_1b_6_a	whole	medium zonated	0.3648	±0.0483
Fig. 03A	To-1(1)	100301_1c_3_b	core	light zonated	0.6426	±0.0353
Fig. 03A	To-1(1)	100301_1e_6_a	rim	light zonated	0.2545	±0.0087
Fig. 03B	To-1(1)	100301_1a_4_b	rim	medium zonated	0.2421	±0.0373
Fig. 03B	To-1(1)	100301_1b_1_a	rim	medium (dark) zonated	0.2481	±0.0112
Fig. 04	To-1(2)	100301_2a_1_b	core	dark	0.3524	±0.0440
Fig. 04	To-1(2)	100301_2a_4_a	rim	medium zonated	0.3636	±0.0626
Fig. 04	To-1(2)	100301_2a_8_a	core, rim	light zonated	0.2767	±0.0411
Fig. 04	To-1(3)	100316_3_c_08_A_low ratios	core	dark	0.2885	±0.0165
Fig. 04	To-1(3)	100316_3_c_10_A	rim + core	medium zonated	0.3547	±0.0413
Fig. 05	To-2	100317_8_A_04_A_low	whole	dark-medium zonated	0.3933	±0.1606
Fig. 05	To-2	100317_8_C_06_A_low	whole	dark-medium zonated	0.3011	±0.0917
Fig. 05	To-2	100317_8_D_06_A_low	whole	dark	0.4025	±0.0399
Fig. 05	To-3	100317_7_A_05_A	whole	dark	0.3332	±0.1117
Fig. 05	To-3	100317_7_B_06_A	rim	dark zonated	0.5577	±0.2576
Fig. 05	To-3	100317_7_D_04_A	rim	dark zonated	0.4099	
Fig. 06	To-5	100316_4_A_06_A	core	medium zonated	0.3274	±0.0244
Fig. 06	To-5	100316_4_A_07_A	core	light	0.3080	±0.1303
Fig. 06	To-5	100316_4_A_10_A	core	medium zonated	0.3824	±0.0404
Fig. 06	To-5	100316_4_B_02_A	core	dark	0.3838	±0.1408
Fig. 06	To-5	100316_4_c_08_A	core	medium zonated	0.3534	±0.0222
Fig. 06	To-5	100316_4_d_03_A	rim + core	medium zonated	0.2461	
Fig. 07	BüMel	100317_11_A_4_A_low	rim	medium zonated	0.9884	±0.3217
Fig. 07	BüMel	100317_11_A_6_A	rim	zonated medium	0.2864	±0.1200
Fig. 07	BüMel	100317_11_B_3_A	whole	zonated medium	0.2527	±0.0344
Fig. 07	BüMel	100317_11_B_5_A	core + (rim)	dark	0.4997	±0.0965
Fig. 07	BüMel	100317_11_C_5_A_low	core + (rim)	dark	0.3478	±0.0197
Fig. 07	BüMel	100317_11_D_9_A_low	rim	light zonated	0.3549	±0.0532
Fig. 07	BüMel	100317_11_E_2_A_low	whole	zonated medium	0.2573	±0.0366
Fig. 07	BüMel	100317_11_E_5_A	core	dark	0.3422	±0.1329
Fig. 07	BüMel	100317_11_E_7_A_high	rim	medium zonated	0.8555	±0.3447

206Pb238U	2 σ	207Pb206Pb	2 σ
0.0391	±0.0024	0.0666	±0.0077
0.0787	±0.0035	0.0587	±0.0013
0.0357	±0.0010	0.0529	±0.0010
0.0326	±0.0031	0.0548	±0.0062
0.0332	±0.0008	0.0546	±0.0021
0.0385	±0.0038	0.0663	±0.0033
0.0372	±0.0022	0.0706	±0.0105
0.0378	±0.0051	0.0542	±0.0023
0.0363	±0.0013	0.0582	±0.0019
0.0348	±0.0021	0.0720	±0.0062
0.0363	±0.0150	0.0806	±0.0075
0.0351	±0.0104	0.0606	±0.0065
0.0366	±0.0021	0.0780	±0.0037
0.0320	±0.0115	0.0780	±0.0170
0.0320	±0.0097	0.1320	±0.0609
0.0426		0.0682	
0.0362	±0.0019	0.0649	±0.0028
0.0383	±0.0117	0.0583	±0.0082
0.0377	±0.0020	0.0725	±0.0060
0.0458	±0.0165	0.0626	±0.0026
0.0360	±0.0016	0.0718	±0.0035
0.0329		0.0560	±0.0033
0.0385	±0.0148	0.1878	±0.0292
0.0314	±0.0119	0.0670	±0.0107
0.0342	±0.0038	0.0537	±0.0042
0.0385	±0.0037	0.0938	±0.0154
0.0341	±0.0010	0.0712	±0.0033
0.0333	±0.0053	0.0729	±0.0041
0.0321	±0.0041	0.0560	±0.0055
0.0336	±0.0084	0.0705	±0.0125
0.0404	±0.0190	0.1594	±0.0288

±

Table 02

	Chemical composition									
SAMPLE	**To-1**	**To-2**	**To-3**	**To-4**	**To-5**	**Mel**	**BüMe l**	**SLO1**	**SLO2**	**To-2**
SiO_2	57.10	70.90	70.80	72.29	76.50	75.50	61.00	73.66	80.70	73.72
TiO_2	0.19	0.16	0.14	0.15	0.17	0.18	0.32	0.34	0.33	0.17
Al_2O_3	10.60	15.40	14.05	14.18	12.65	13.00	10.65	15.49	10.68	16.01
Fe_2O_3	0.54	2.11	1.95	2.21	1.41	1.88	3.07	2.59	1.84	2.19
MnO	0.22	2.72	3.17	2.66	0.65	1.16	1.54	0.04	0.01	2.83
MgO	0.04	0.01	0.04	0.02	0.01	0.01	0.06	0.60	0.27	0.01
CaO	13.50	0.67	1.17	0.90	0.30	0.10	8.73	0.10	0.04	0.70
Na_2O	5.88	1.40	1.38	1.41	4.16	1.40	4.04	3.84	1.62	1.46
K_2O	0.09	2.67	2.72	2.28	2.20	4.27	1.04	3.22	4.43	2.78
P_2O_5	0.09	0.11	0.09	0.10	0.11	0.02	0.09	0.07	0.02	0.11
SrO	0.03	0.01	0.01	0.01	0.01	<0,01	0.03			0.01
Cr_2O_3	<0,01	<0,01	<0,01	<0.002	<0,01	<0,01	<0,01			
BaO	<0,01	0.02	0.02	0.01	0.01	0.03	0.01	0.05	0.05	0.02
LOI	10.70	4.10	4.68	3.7	1.72	2.49	8.71			
Total	98.99	100.28	100.20	99.92	99.89	100.01	99.26	100.36	100.79	100.00
Na_2O plus K_2O										4.23

without LOI, recalcualted to 100%					
To-3	**To-4**	**To-5**	**Mel**	**SLO1**	**SLO2**
74.12	75.13	77.93	77.42	73.66	80.70
0.15	0.16	0.17	0.18	0.34	0.33
14.71	14.74	12.89	13.33	15.49	10.68
2.04	2.30	1.44	1.93	2.59	1.84
3.32	2.76	0.66	1.19	0.04	0.01
0.04	0.02	0.01	0.01	0.60	0.27
1.22	0.94	0.31	0.10	0.10	0.04
1.44	1.47	4.24	1.44	3.84	1.62
2.85	2.37	2.24	4.38	3.22	4.43
0.09	0.10	0.11	0.02	0.07	0.02
0.01	0.01	0.01			
0.02	0.01	0.01	0.03	0.05	0.05
100.02	100.00	100.01	100.03	100.00	100.00
4.29	3.83	6.48	5.81	7.06	6.06

Table 03

	Rhyolite clasts from Middle Jurassic olistostrome							T3 in situ samples from the Slovenian Trough	
Element	**To-1**	**To-2**	**To-3**	**To-4**	**To-5**	**Mel**	**BüMel**	**SLO1**	**SLO2**
Cs	0.31	4.87	4.66	4.30	3.34	5.82	1.64	9.79	7.3
Rb	3.00	124.00	133.50	99.70	109.50	174.50	37.90	136.5	120.5
Ba	22.00	146.50	185.50	109.00	67.20	282.00	83.10	394	421
Th	13.60	14.30	13.75	13.40	14.00	21.10	13.70	20.7	16
U	2.26	5.54	4.01	5.00	2.74	5.23	1.47	4.65	3.05
Nb	8.60	11.60	11.50	9.60	9.40	16.50	7.60	10.9	9.5
Ta	1.00	1.50	1.50	1.20	1.60	1.60	0.90	0.9	0.8
La	17.10	13.90	10.40	11.10	13.40	49.50	26.80	47.9	41.8
Ce	36.60	32.90	24.40	28.20	30.60	104.00	60.80	87.5	76.6
Pr	4.78	3.90	3.05	3.29	3.75	11.85	7.49	10.5	9.14
Sr	217.00	99.30	66.80	86.50	58.70	26.50	238.00	32.6	31.5
Nd	18.30	14.90	11.40	13.20	13.80	45.40	30.90	39.6	34.5
Zr	112.00	102.00	98.00	92.20	107.00	186.00	180.00	263	152
Hf	3.20	3.40	3.20	3.20	3.40	6.10	5.50	7	4.1
Sm	4.05	4.59	3.67	3.50	3.53	8.65	6.07	8.29	6.13
Eu	0.34	0.39	0.22	0.32	0.21	0.83	0.97	0.79	0.58
Gd	4.36	4.66	4.14	4.25	3.94	8.04	5.54	6.69	4.54
Tb	0.78	1.00	0.90	0.91	0.78	1.31	0.84	1.07	0.76
Dy	5.20	6.85	6.19	6.40	5.12	8.09	4.94	6.36	4.49
Ho	0.99	1.38	1.23	1.26	1.06	1.62	0.95	1.37	0.9
Er	3.25	4.35	3.69	3.80	3.20	4.93	2.82	4.08	3
Tm	0.44	0.63	0.56	0.61	0.45	0.70	0.39	0.61	0.44
Yb	3.00	4.06	3.52	3.63	2.90	4.78	2.93	3.7	2.93
Y	29.30	42.90	35.80	36.00	29.60	44.70	26.70	38	25.9
Lu	0.42	0.56	0.48	0.53	0.43	0.69	0.46	0.58	0.47
Ga	5.50	23.40	21.30	18.50	17.90	19.70	9.40	18.3	12.5
V	8.00	6.00	8.00	9.00	8.00	9.00	32.00		
Cr	10	below det.	below det.	10	10	below det.	10		